geologicaacta

Citation: Jaime Urrutia-Fucugauchi1,2, Ligia Perez-Cruz1,2,3, Rafael Venegas-Ferrer1, Pablo Sanchez-Solis, 2025.The Chicxulub Crater Drilling Program – Continuous Coring, Well Logging and Core Analyses Reviewed. Geologica Acta, 23.3, 1-21.

Online ISSN: 1696-5728 DOI: 10.1344/GeologicaActa2025.23.3

The Chicxulub Crater Drilling Program – Continuous Coring, Well Logging and Core Analyses Reviewed

Jaime Urrutia-Fucugauchi[1,2] Ligia Perez-Cruz[1,2,3] Rafael Venegas-Ferrer[1] Pablo Sanchez-Solis[2]*

[1] Programa Universitario de Perforaciones en Océanos y Continentes, Instituto de Geofísica. Universidad Nacional Autónoma de México
Coyoacan 04510 Mexico

[2] Instituto de Investigación Científica y Estudios Avanzados Chicxulub, Parque Científico y Tecnológico de Yucatán
Sierra Papacal, Mérida, Yucatan 97302, Mexico

[3] Coordinación de Plataformas Oceanográficas, Coordinación de la Investigación Científica, Universidad Nacional Autónoma de México
Coyoacan 04510, Mexico

* Present Address: PEMEX Exploración Producción, Petróleos Mexicanos, Villahermosa, Tabasco, México

ABSTRACT

Continuous core recovery, core scanning and logging are used for borehole characterization and petrophysical analyses in the Chicxulub drilling projects. The crater formed by an asteroid impact on the Yucatan platform ~66Ma ago, marking the Cretaceous/Paleogene (K/Pg) boundary. The K/Pg boundary clay layer, characterized by the Ir and platinum group element anomaly, has been studied worldwide. The crater has a ~200km rim diameter and is covered by up to ~1 km of carbonate sediments, with studies based on geophysical surveys, drilling and ejecta deposits. The Yaxcopoil-1 borehole, drilled in the southern crater terrace zone sampled the post-impact carbonates, impact breccias and target Cretaceous carbonates. The M0077A borehole drilled in the marine sector sampled the peak ring succession, with the post-impact carbonates, impact breccias, melt and basement. The Yaxcopoil-1 and M0077A boreholes were continuously cored from about 400m to 1511 and 1335m, respectively and sampled distinct crater structures. Studies provide constraints on the crater formation, crustal deformation, lateral/vertical displacement, ejecta emplacement and crater collapse. Impact breccias are heterogeneous materials, with clasts of melt, carbonates and basement in carbonate-rich and melt-rich matrix. The lower breccias were emplaced by high-temperature basal surges, followed by collapse of the impact plume and lateral curtains. The upper breccias are reworked deposits of the post-collapse stage. The crater formed a depositional basin, filled with sediments that preserve records of sea level and sediment transport across the platform. Core analyses and scans provide constraints on the structure, stratigraphy, textures, mineralogy, deformation and hydrothermal alteration. Studies show the usefulness of continuous coring and core analyses to constrain the crater formation, impact deformation, ejecta and impact dynamics.

KEYWORDS **Chicxulub crater, Yaxcopoil-1 borehole, Post-impact carbonates, Impactites, Target carbonates, Core analysis, Physical properties, Yucatan, Gulf of Mexico**

INTRODUCTION

Drilling is a major component of research projects and oil and mineral exploration programs. Integration of drilling with geophysical-geological surveys and modelling has expanded the resolution and capabilities to investigate underground structures (Chapman, 2000; Moon *et al.*, 2006; National Research Council, 1994; Selley, 1998). The international drilling programs in the 1960's and 1990's have contributed to the understanding of the Earth system and to technological developments (Ashena and Thonhauser, 2018; Becker *et al.*, 2019; Harms and Emmermann, 2017; Revelle, 1981). In the past decades, riser and non-riser drilling platforms, directional drilling, core scans and automatization have permitted drilling deeper and in complex geological settings (Becker and Davis, 2005; Yamada *et al.*, 2019).

The international ocean and continental drilling programs integrate extensive logging and core recovery providing a wealth of data and samples (Becker *et al.*, 2019; Harms and Emmermann, 2017; Shouting and Wentao, 2022). Core analyses include digital scans, physical properties, petrology, mineralogy, geochemistry, isotopes and biostratigraphy. Recent developments include a wide range of filters, computer tomography CT scans and supervised/unsupervised processing tools (Conze *et al.*, 2007; Conze, 2016; Smith *et al.*, 2020). The X-ray CT scans provide high-resolution for lithological core characterization (Akin and Kovseck, 2003; Freifeld *et al.*, 2006; Tanaka *et al.*, 2011; Tonai *et al.*, 2016). The advent of semi-automatic core scans with uniform geometries, light control and core handling provides homogenous high-resolution data that integrate with logs and discrete measurements.

Chicxulub crater is a large multiring structure formed ~66Ma ago by an asteroid impact on the Yucatan carbonate platform in the southern Gulf of Mexico (Fig. 1). The impact is associated with the End-Cretaceous mass extinction at the Cretaceous/Paleogene (K/Pg) boundary (Alvarez *et al.*, 1980; Schulte *et al.*, 2010). The crater is covered by post-impact carbonates up to ~1km in the central crater zone, with studies based on geophysical surveys, drilling and modeling (Collins *et al.*, 2020; Duong *et al.*, 2023; Gulick *et al.*, 2013; Hildebrand *et al.*, 1991, 1998; Perez-Cruz and Urrutia-Fucugauchi, 2024; Sharpton *et al.*, 1992, 1993; Urrutia-Fucugauchi *et al.*, 2011, 2022). The boreholes have sampled the impactite rocks and the post- and pre-impact sedimentary sequences, critical for constraining the structure formation and age.

Here we review the use and applications of continuous coring, core scanning and logging, with reference to the Chicxulub drilling projects (Fig. 2). The boreholes sampled the impactites, the post- and pre-impact sequences and the basement. Inside the crater, the Yaxcopoil-1 borehole drilled the terrace zone near the crater southern rim and the M0077A borehole drilled the peak ring succession in the marine sector (Fig. 3).

CHICXULUB IMPACT CRATER

In the early stages of planetary evolution, impacts were involved during the formation of the planetary bodies, including large-scale collisions such as the one with the Earth forming the Moon (Aspaugh, 2014). The terrestrial record of crater-forming impacts has been modified by the dynamic processes of tectonics, volcanism and erosion (Kenkmann, 2021; Kenkmann *et al.*, 2014; Melosh, 1989; Melosh and Ivanov, 1999; Urrutia-Fucugauchi and Perez-Cruz, 2008). Large complex impact structures documented include the Vredefort, Sudbury and Chicxulub, with the latest being the youngest and best preserved.

Chicxulub crater formed ~66Ma ago by an asteroid impact on the Yucatan carbonate platform. The crater is characterized by high amplitude gravity and magnetic anomalies (Hildebrand *et al.*, 1991, 1998; Sharpton *et al.*, 1993). The gravity anomaly shows a ring pattern with a central high, multiring morphology and the central uplift. Chicxulub has been studied with a range of methods, including gravity, magnetics, magnetotellurics and seismics (*e.g.* Morgan *et al.*, 1997, 2016; Delgado-Rodriguez *et al.*, 2001; Urrutia-Fucugauchi *et al.*, 2011, 2022; Batista *et al.*, 2013; Gulick *et al.*, 2008, 2013; Christeson *et al.*, 2021).

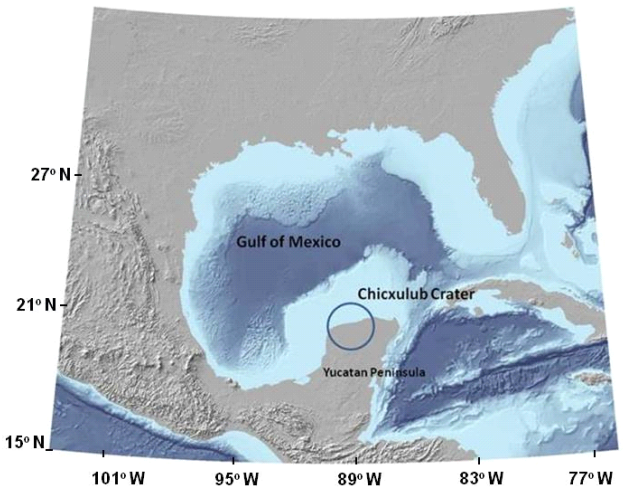

FIGURE 1. Location of Chicxulub crater in the Yucatan peninsula and southern Gulf of Mexico (base map after French and Schenk, 2004). Inset: Satellite radar interferometry image of the Yucatan peninsula (credit NASA Jet Propulsion Laboratory). The buried crater is marked on the surface by a semicircular ring of cenotes and a topographic depression. Also shown are past coastlines and the Ticul fault (Urrutia-Fucugauchi *et al.*, 2008).

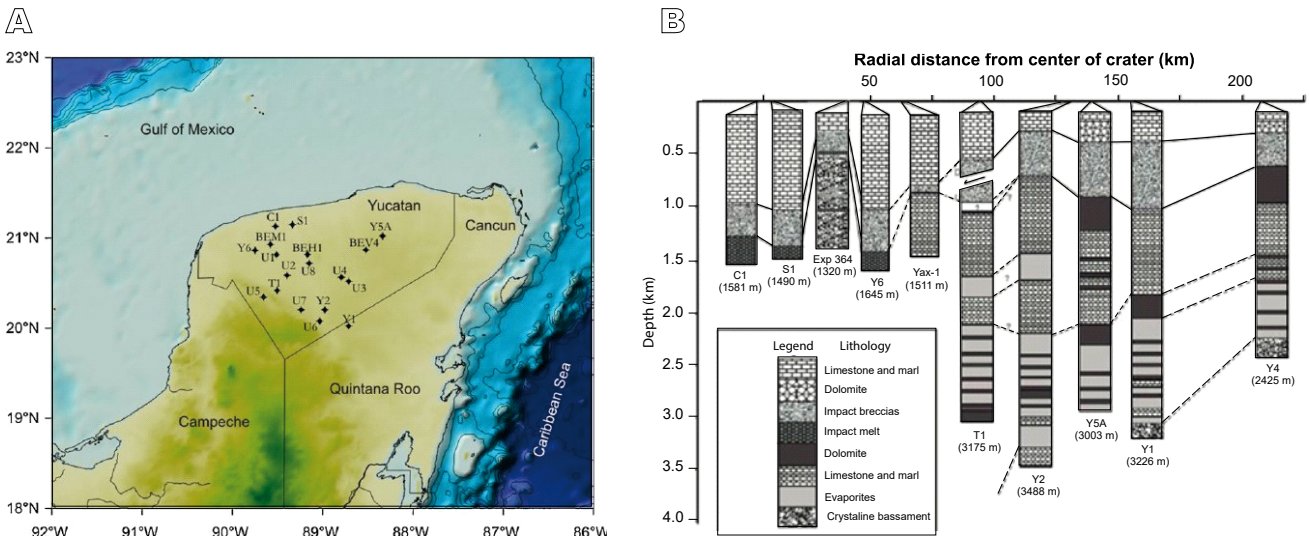

FIGURE 2. A) Drilling sites in northwestern Yucatan. B) Schematic borehole columns, plotted as a function of distance to the Chicxulub crater center at Chicxulub Puerto on the coastline (Lopez Ramos, 1976; Urrutia-Fucugauchi *et al.*, 2004, 2011; Morgan *et al.*, 2016).

The impact excavated and fragmented deep into the crust of the target area, forming a transient cavity (Collins *et al.*, 2008, 2020). The fragmented material was ejected at high temperature and velocity, forming a central plume and lateral curtains, with ejecta reaching large distances with a global distribution (Alvarez *et al.*, 1980; Artemieva and Morgan, 2020; Schulte *et al.*, 2010). Proximal ejecta deposits have been found at outcrops in Belize, southern and northeastern Mexico and USA and the Caribbean (Pope *et al.*, 2005).

The drilling projects with continuous core recovery are conducted to investigate the structure and stratigraphy in the crater zone (Fig. 2). The 1994-1996 drilling program included eight boreholes in the central and southern sectors and drilled into the carbonates and impactite sequence (Urrutia-Fucugauchi *et al.*, 1996). In the southern sector, three boreholes cut the impact breccias, documenting the inverted stratigraphy with the lower carbonate-rich breccias and the upper basement and melt-rich breccias. The eastern crater sector was studied in the Federal Commission of Electricity (CFE)-UNAM drilling project, with three boreholes in the Valladolid region (Urrutia-Fucugauchi *et al.*, 2008). The marine sector was drilled as part of the International Ocean Discovery Program (IODP)-International Continental Drilling Program (ICDP) Expedition 364 with the M0077A borehole on the peak ring (Morgan *et al.*, 2016).

The Yaxcopoil-1 borehole was drilled as part of the Chicxulub Drilling Program (CSDP) of the International Continental Scientific Drilling Program and National University of Mexico (Urrutia-Fucugauchi *et al.*, 2004). The borehole drilled through the down faulted blocks of the terrace zone. The objective was to core continuously into the post-impact sediments and through the impact breccias and the target section.

The M0077A borehole drilled the offshore section of the peak ring, through the post-impact carbonates, the impact breccias, melt and the basement. The peak rings are semicircular structures with an elevated relief over the crater floor. The drilling project aimed to investigate the formation mechanism and unraveling its deep structure (Morgan *et al.*, 2016). The occurrence of granitic rocks at shallow depths beneath the impactites supports formation models involving basement uplift, with vertical/lateral transport of crustal material forming the peak ring structure (Baker *et al.*, 2016; Collins *et al.*, 2020).

The analyses of well logs and cores allow to characterize the lithology, petrography, physical properties, geochemistry, isotopes, biostratigraphy, magnetostratigraphy, shock deformation and hydrothermal system under the terrace zone (Arz *et al.*, 2004; Gelinas *et al.*, 2004; Kring *et al.*, 2004; Lüders and Rickers, 2004; Pilkington *et al.*, 2004; Rowe *et al.*, 2004; Wittmann *et al.*, 2004) and the peak ring (Christeson *et al.*, 2018; Gulick *et al.*, 2017; McCall *et al.*, 2020; Morgan *et al.*, 2016; Whalen *et al.*, 2020).

METHODS AND RESULTS

The Yaxcopoil-1 borehole was drilled from December 2001 through March 2002 at a site ~62km radial distance from the approximate crater center at Chicxulub Puerto

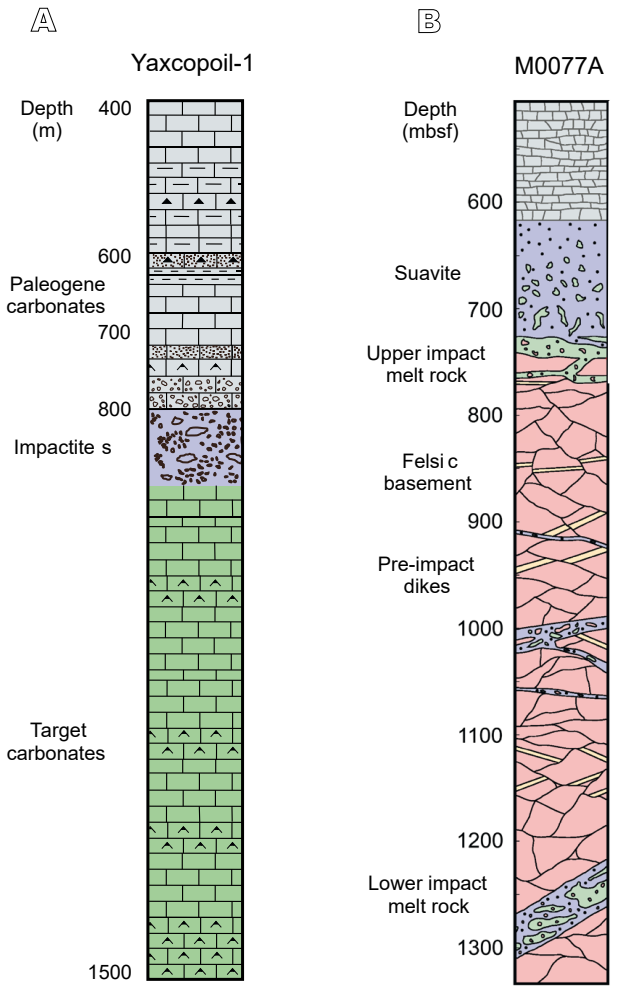

FIGURE 3. A) Location on the Yaxcopoil-1 and M0077A drilling sites on the terrace zone and peak ring. B) Yaxcopoil-1 schematic column, with the Paleogene carbonates, impact breccias and Cretaceous target section (Wohlgemuth *et al.*, 2004). C) Borehole column for the M0077A well (Morgan *et al.*, 2016).

(Fig. 3). The drill site was selected based on gravity, aeromagnetic and magnetotelluric surveys, with constraints from offshore seismic surveys and the Pemex and Chicxulub borehole data (Urrutia-Fucugauchi *et al.*, 2004, 2011).

An INDECO rotary drill rig from Perforaciones Industriales Termicas, S.A. PITSA and a core recovery system from the Drilling, Observation and Sampling of the Earth's Continental Crust (DOSECC) were used (Fig. 4). The rotary mode was used from surface to 404m depth. This section was wireline logged and cased. Then, drilling continued with wireline coring of the Paleogene sequence, impactites and Cretaceous section. Cores with 63.5mm diameter were obtained to a depth of 993m. At this depth, the HQ coring string became stuck, and was left in the hole as casing. The wireline coring was reassumed with an NQ string with core diameter of 47.6mm to a final depth of 1511m.

The logging was completed in two stages, the first down to 400m and at the end of the drilling phase down to 1511m (Wohlgemuth *et al.*, 2004). The gamma ray, electrical dual lateralog (DLL) deep and DLL shallow resistivity, low-field magnetic susceptibility and sonic compressional Vp velocity logs were acquired. Gamma ray and sonic logs were acquired between 400 to 993m (Wohlgemuth *et al.*, 2004). Additionally, downhole temperature gradients were measured to investigate and monitor the thermal state (Popov et al, 2004, 2011).

The Yaxcopoil-1 borehole was continuously cored from 404m to 1511m depth, with core recovery of 98.5%. The 3m long core runs were split, marked and stored in boxes at the drilling site (Fig. 5). Cores were marked and digitally scanned during the drilling operation. In the Chicxulub Core Repository, cores were cut in halves and re-scanned. Core analyses include petrological, geochemical, petrophysical, geochronological, thermal conductivity, magnetic properties, seismic velocities and elastic properties (Ebra and Pesonen, 2014; Kenkmann et al, 2004; Keppie *et al.*, 2011; Kring *et al.*, 2004; Mayr *et al.*, 2008; Popov *et al.*, 2011; Schmieder *et al.*, 2018; Urrutia-Fucugauchi *et al.*, 2004, 2014; Whalen *et al.*, 2013).

The core boxes were labelled in a consecutive downhole sequence and photographed. The core recovery rate and initial macroscopic descriptions were recorded. The macroscopic core descriptions, with the textures, lithology, colors, bedding and structural features were recorded and a preliminary lithological column prepared.

In the Chicxulub repository, cores were cut in halves, re-marked and digitally scanned in the smartCIS 1600 line core scanner (smartcube GmbH – Information Management Systems). The system provides high resolution 3-D and 2-D core images (from 250 up to 1000dpi DOF Depth-Of-Field mode), with maximum scan lengths of 160cm and core diameters up to 20cm. For the core analyses, a 500dpi was used, with core color records corrected for the R, G and B components and a standardized color calibration. The archive core halves are documented and stored in the Chicxulub Core Repository (Fig. 6). Physical property logging on the cores with non-invasive tools for magnetic susceptibility, density, and geochemistry are conducted.

The M0077A borehole was drilled on the marine sector at the intersection of two seismic lines, to investigate the peak ring structure and stratigraphy (Morgan *et al.*, 2016). The seismic lines were acquired as part of the Chicxulub Seismic Experiment (Morgan *et al.*, 2005). Two prospect drilling sites were selected for further study. The site characterization for the M0077A borehole was later analyzed with detailed multibeam bathymetric surveys and geotechnical studies (Goff *et al.*, 2016).

FIGURE 4. Drilling of the Yaxcopoil-1 borehole, Chicxulub Drilling Project. Views of the drill rig, coring and cores.

FIGURE 5. Chicxulub Drilling Project CSDP. Views of the CSDP Core Repository.

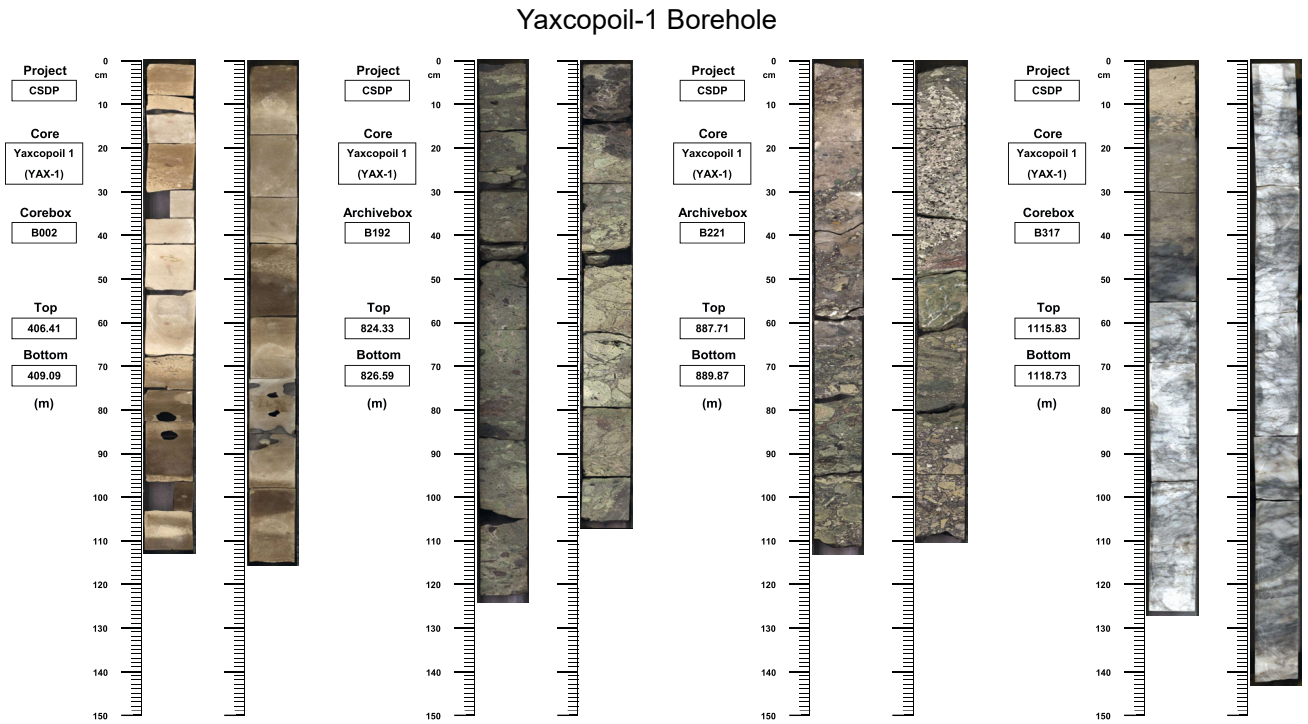

FIGURE 6. A) The Yaxcopoil-1 simplified borehole column (Wohlgemuth *et al.*, 2004). B) Core box images for the post-impact carbonates, impact breccias and target carbonates.

The core analyses were made at the IODP Core Repository of the University of Bremen, cores were split in halves and further described. The science party worked on core characterization and analyses on physical properties, geochemistry, micropaleontology, paleomagnetism, mineralogy and petrology (Morgan *et al.*, 2016). Studies include dual-energy X-ray computed tomography made at the Houston Weatherford Laboratory. The data processing was done at Austin by Enthought, Inc. The X-ray CT scans measure the densities and average atomic numbers for the textural, mineralogical composition and fractures.

For the analysis, core scan images are integrated with geophysical logs, borehole wall images and petrological microscope data on thin and polished sections. The working core halves are used for subsampling and the petrophysics, biostratigraphy, and geochemical and isotope analyses.

Yaxcopoil-1 Borehole

In the Yaxcopoil-1 the post-impact carbonates were cored between 404m and 795m. The impact breccia section was cored between 795m and 895m, which is thinner compared to thickness of the breccias drilled in the Pemex and Chicxulub wells (Urrutia-Fucugauchi *et al.*, 1996, 2008, 2011). The target carbonate sequence was cored from 895m to 1511m (Fig. 3). The core analyses include macroscopic descriptions, orientation marking, digital core scans and physical/chemical properties.

The post-impact sequence is formed by calcareous breccias, limestones, lutites, argillaceous limestones, calcarenites with microcrystalline nodules, wackestones with bioclasts, evaporates and salt precipitates, silicified limestones, calcareous cherts and marls (Fig. 7). The bedding plane dips from sub-horizontal up to 60 degrees. Sedimentary structures include cross-lamination, current-flow features, parallel lamination, cyclic graded bedding and styolitic structures. Conglomerate layers with clasts of limestones and evaporites and gravity flows are characteristic in the succession. From the thin-section petrographic observations, two microfacies were identified. Facies 1 varies from mudstone to wackestone and facies 2 varies from wackestone to packstone. The changes in textures, compositions and sedimentary structures characterize twelve lithostratigraphic units along the column (Figs. 3; 4).

The carbonates were deposited in low-energy deep bathyal environments, with characteristic fine-grained facies varying from mudstone to wackestone. The carbonate breccias with intercalated fine-grained gravity flow deposits represent deposits transported from shallower zones to the deeper zones inside the basin, marked by

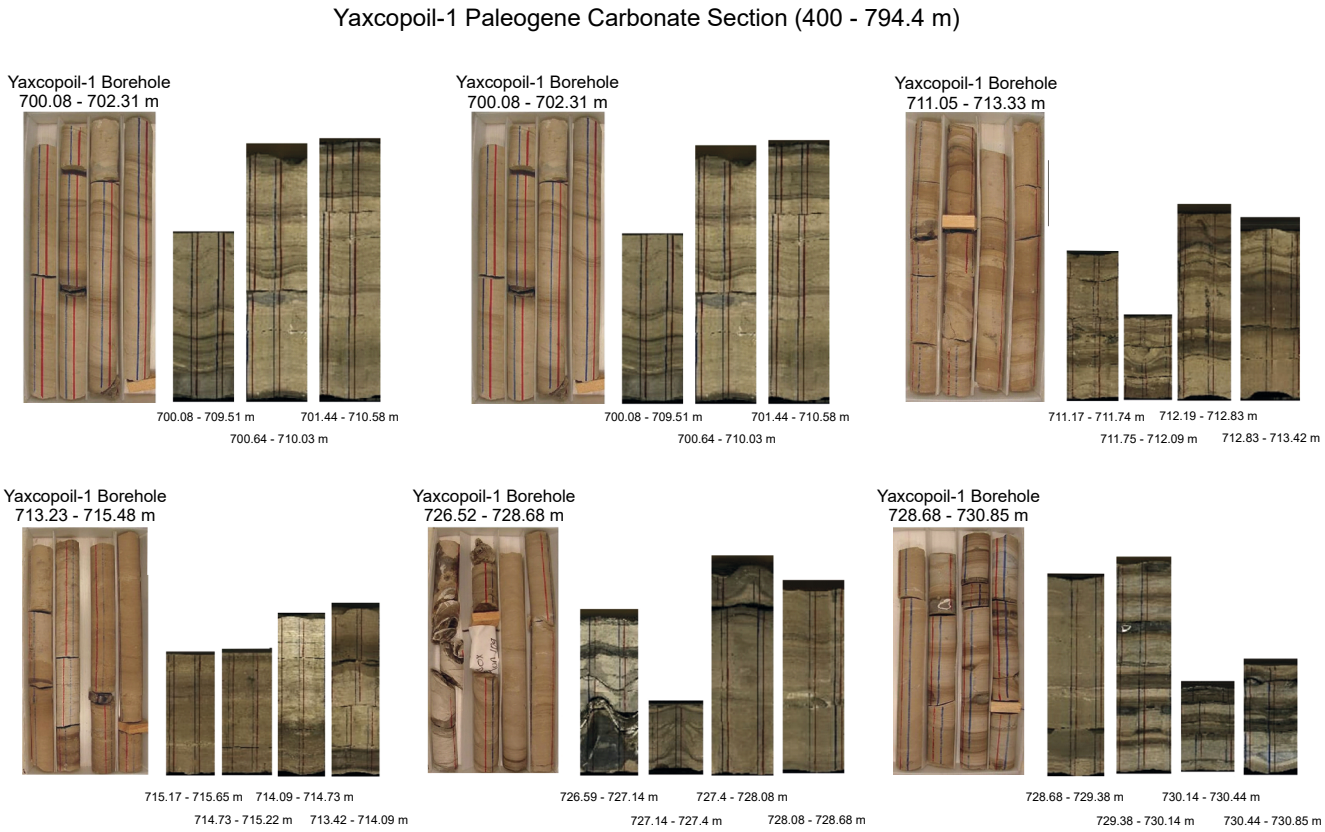

FIGURE 7. Post-impact carbonate section cored between 400 to 797.4m depth. Cores have been digitally scanned, with core box images and 3-D images.

changes in textures and grain sizes from grainstone to packstone. The upper units are characterized by microfacies varying from wackestone to packstone with planktic and benthonic foraminifera and bioclasts. Some units show an increase in silicification, with replacing clasts and fossils and microcrystalline quartz flows. Some show laminated rhythmic clay layers, with a thick section formed by laminated black shales and lighter marls.

The impactite section is ~100m thick, formed by six units (Fig. 8). i) Upper Sorted Suevite (USS) (794-808m), ii) Lower Sorted Suevite (LSS) (808-823 m), iii) Upper Suevite (US) (823-846m), iv) Middle Suevite (MS) (846-861m), v) Brecciated Impact Melt Rock (BMR) (861-885m) and vi) Lower Suevite (LS) (885-895m) (Kring *et al.*, 2004; Stöffler *et al.*, 2004; Tuchscherer *et al.*, 2004). The breccias are heterogeneous with distinct clast and matrix compositions and degree of alteration.

The basal carbonate section is formed by limestones, calcarenites, dolomite breccias, anhydrites and paraconglomerates, cut by melt, suevite and clastic dykes (Fig. 9). The section shows effects of hydrothermal alteration and is cut by thin breccias, melt and clastic dykes (Rowe *et al.*, 2004; Wittmann *et al.*, 2004). The anhydrite layers vary from a few centimeters to up to 15m thick form some 27% of the sequence. An organic matter-rich and oil-bearing impregnated interval is present in the lower section (Kenkmann *et al.*, 2004; Lüders and Rickers, 2004).

The M0077A Borehole

The M0077A borehole was drilled over the peak ring from the L/B Myrtle mission specific platform. It drilled the peak ring succession formed by post-impact carbonates (0-618m), impact suevites and clast-poor melt (618-748m) and the basement section of granites and dykes (Fig. 3). Continuous coring was from 505.7m to 1335.7m. Logs were acquired in three phases with the caliper, acoustic and optical images, fluids, electrical resistivity, induction conductivity, magnetic susceptibility, sonic and gamma rays.

Core analyses include density, porosity, mineralogy, petrology, magnetic susceptibility, seismic velocities, microfossils (Gulick *et al.*, 2017; Morgan *et al.*, 2017). Dual-energy X-ray computed tomography provided data on textures, composition and fracturing.

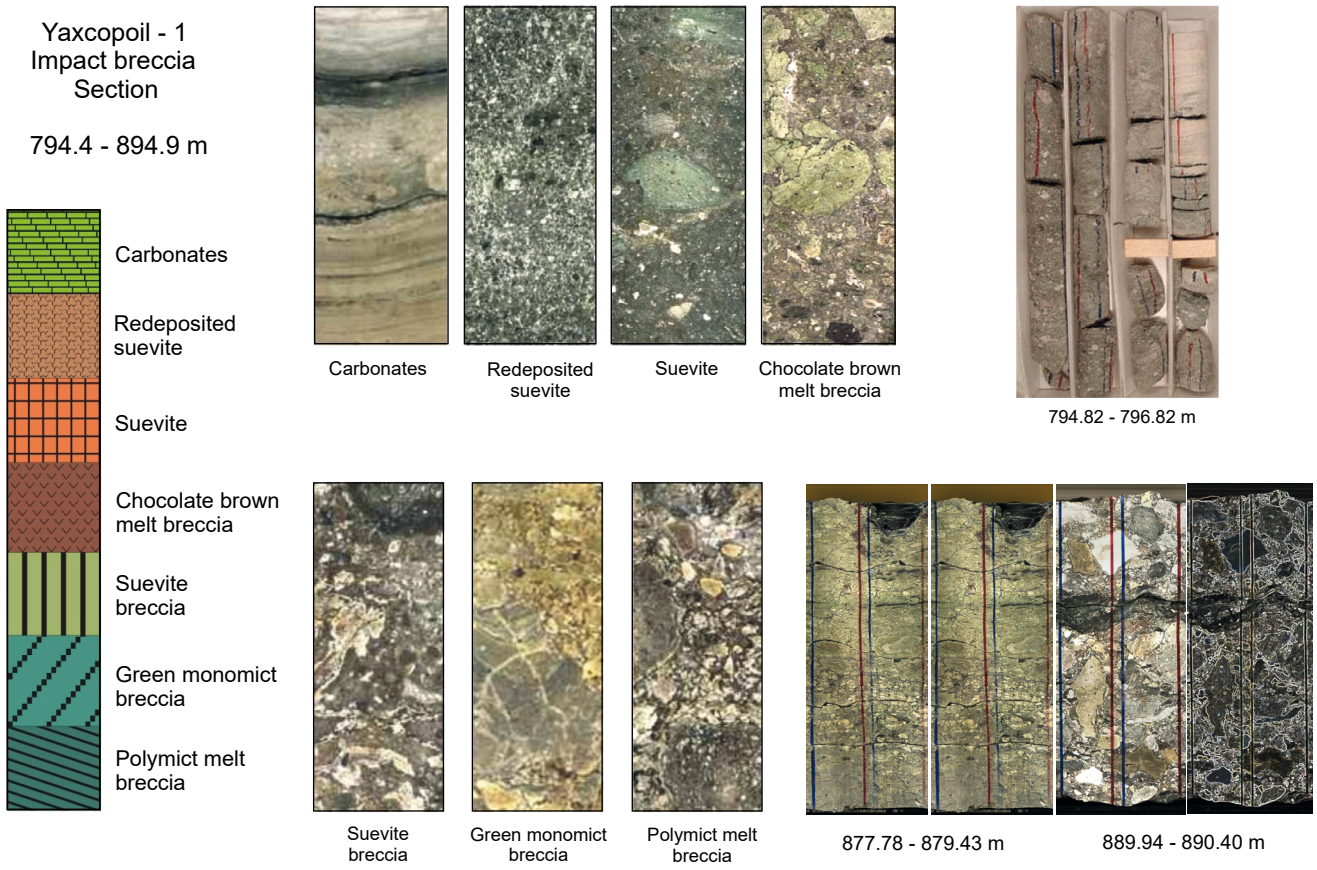

FIGURE 8. Impact breccia section and carbonate-breccia contact. The breccia section, cored between 794.4-894.9m depth, is divided into six units (Urrutia-Fucugauchi *et al.*, 2004). 3-D core images, core box with the carbonate-breccia contact and petrographic images of the breccia units.

The carbonate-impactites contact at 748m is marked by high magnetic susceptibility and gamma ray values. The granites are intensely fractured and deformed, with foliated shear zones and cataclasites, and cut by pre-impact and impact dikes (Christeson *et al.*, 2018; Gulick *et al.*, 2017).

DISCUSSION

Core scans and physical property logs provide constrains on the impactite lithologies and post- and pre-impact carbonate sequences. The lithostratigraphic units correlate with the physical property logs, including magnetic susceptibility, density, Vp seismic velocity and geochemical logs (Figs. 10; 11; 12). Logs display low frequency sinusoidal trends with superimposed high frequency high amplitude fluctuations. The density varies with lithology, with values between 1.7 and 2.6kg/m^3. The Vp seismic velocity log shows a wide range of 2.5 to 6km/s, varying with the lithology and degree of fracturing and deformation.

The impact breccia section is characterized by fracturing and alteration, marked by low densities, low seismic velocities and high porosity (Fig. 10), which are observed in the gravity and seismic velocity models (Christeson *et al.*, 2018). The magnetic susceptibility logs in the carbonate sections show dominant diamagnetic values with small paramagnetic contribution. The logs show small amplitude changes within a narrow range between -0.5 and 5·10^{-5}SI. Variable magnetic susceptibilities are characteristic of the breccias, depending on the relative contents of melt, basement and carbonate clasts and matrix. The basal carbonate sediments above the contact with the breccias show high susceptibilities and high Fe and Ti contents, correlating with the hydrothermal alteration and input from the underlying breccias (Escobar-Sanchez and Urrutia-Fucugauchi, 2010; Rowe *et al.*, 2004).

The impact breccias are highly heterogeneous, with a complex assemblage of basement and melt clasts in melt-rich and carbonate-rich matrix (Fig. 8). The clast distribution and matrix textures, analyzed in the core scan images and logs, vary within and between the units. The basal units were emplaced at high temperatures as basal surges and the upper unit at low temperature showing reworking under aqueous conditions. The physical property logs in the

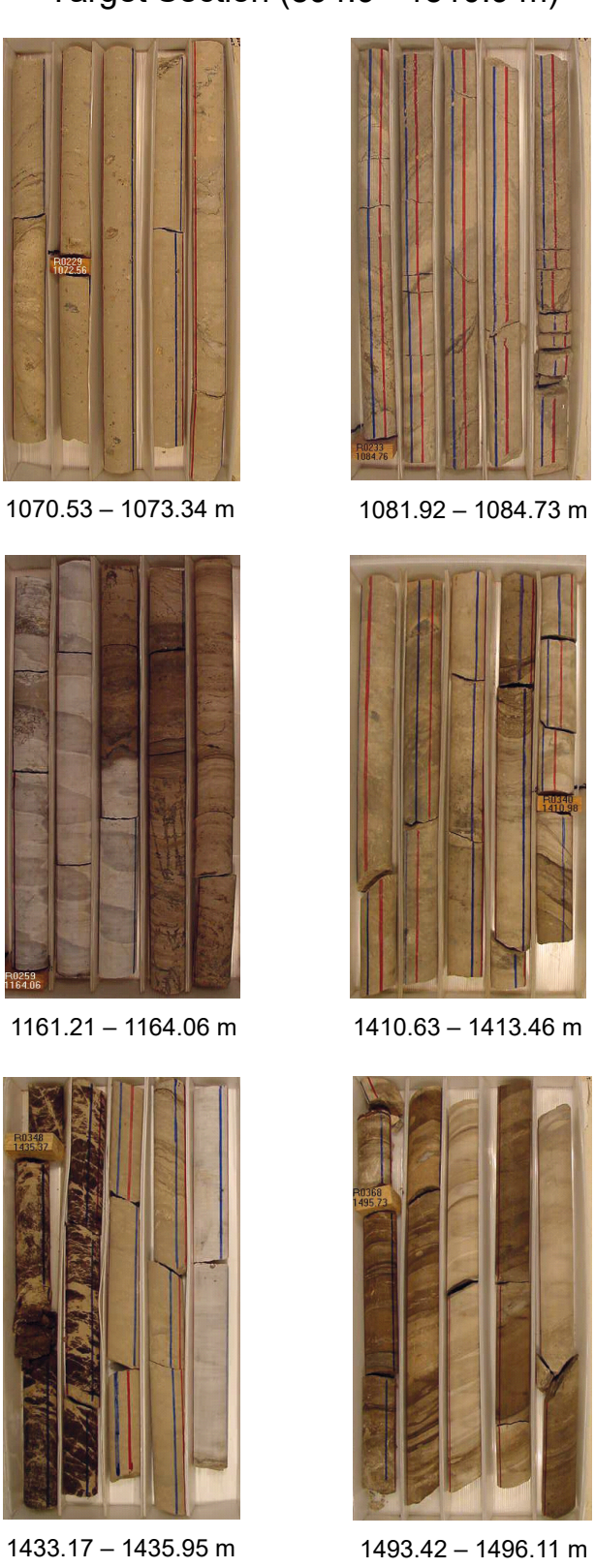

FIGURE 9. The pre-impact target carbonate sequence. Core box images and 3-D core scans of the impact breccia section.

breccia section show distinct trends, corresponding to the distribution and mixtures of carbonate and basement clasts and melt in melt-rich and carbonate-rich matrix (Kring *et al.*, 2004; Urrutia-Fucugauchi *et al.*, 2004, 2014; Stöffler *et al.*, 2004). The magnetic susceptibility logs vary with high values in basement and melt clasts and matrix and low values in carbonate clasts and carbonate-rich matrix (Urrutia-Fucugauchi *et al.*, 2014).

The joint analyses of well and core analyses open interesting opportunities, which require further development. Continuous core recovery programs require extended drilling time and increased costs and the emphasis has been on the use of well logging, coupled with intermittent core recovery. Logging tools were used for the M0077A borehole characterization, physical properties, well condition, fluids and temperature-pressure state (Lofi *et al.*, 2018). Analyses on cores and cuttings provide information on petrology, mineralogy, fossils, fluids, fractures, chemistry, paleomagnetism, isotope geochemistry, which are needed for age control, biostratigraphy, magnetic polarity and isotope stratigraphy, sedimentology, and alteration (Freifeld *et al.*, 2006; Rothwell *et al.*, 2006; Smith *et al.*, 2020; Tanaka *et al.*, 2011; Tonai *et al.*, 2019). In general, well and core logs showed good agreement, providing data for petrophysical characterization, borehole correlations, stratigraphy and structure. When discrepancies arise, they also provide information related to instrumental and measurement effects, fluids, and sensor-borehole wall conditions. Core analyses in the laboratory are under controlled sample-sensor geometries, temperature-pressure and fluids and atmosphere conditions. Well logs provide additional information on the characteristics and properties of the geological formations around the borehole.

In the Chicxulub drilling projects, well logs and core data are used, which allows analyzing the distinct spatial scales and conditions (Christeson *et al.*, 2018; Lofi *et al.*, 2018). The developments in geophysical logging, continuous core recovery tools and core analyses provide better characterization of the lithologies and stratigraphy (*e.g.* Arns *et al.*, 2005; Conze, 2016; Rothwell and Rack, 2006). The usefulness of 3-D core images in documenting the stratigraphy and deformation of the carbonate target sequence is illustrated in the target section (Kenkmann *et al.*, 2004; Figs. 13; 14). Crater collapse stage models show target material deformed and displaced (Collins *et al.*, 2008, 2020). The contrasting allochthonous and para-autochthonous models propose the involving of overturned blocks with an inverted stratigraphy and conformal stratigraphy with laterally displaced blocks of target rocks (Kenkmann *et al.*, 2004; Stöffler *et al.*, 2004). The analyses focus on quantifying the bedding plane attitudes and the fractures based on the 3-D core scan images, with bedding plane attitudes from sub horizontal to steep

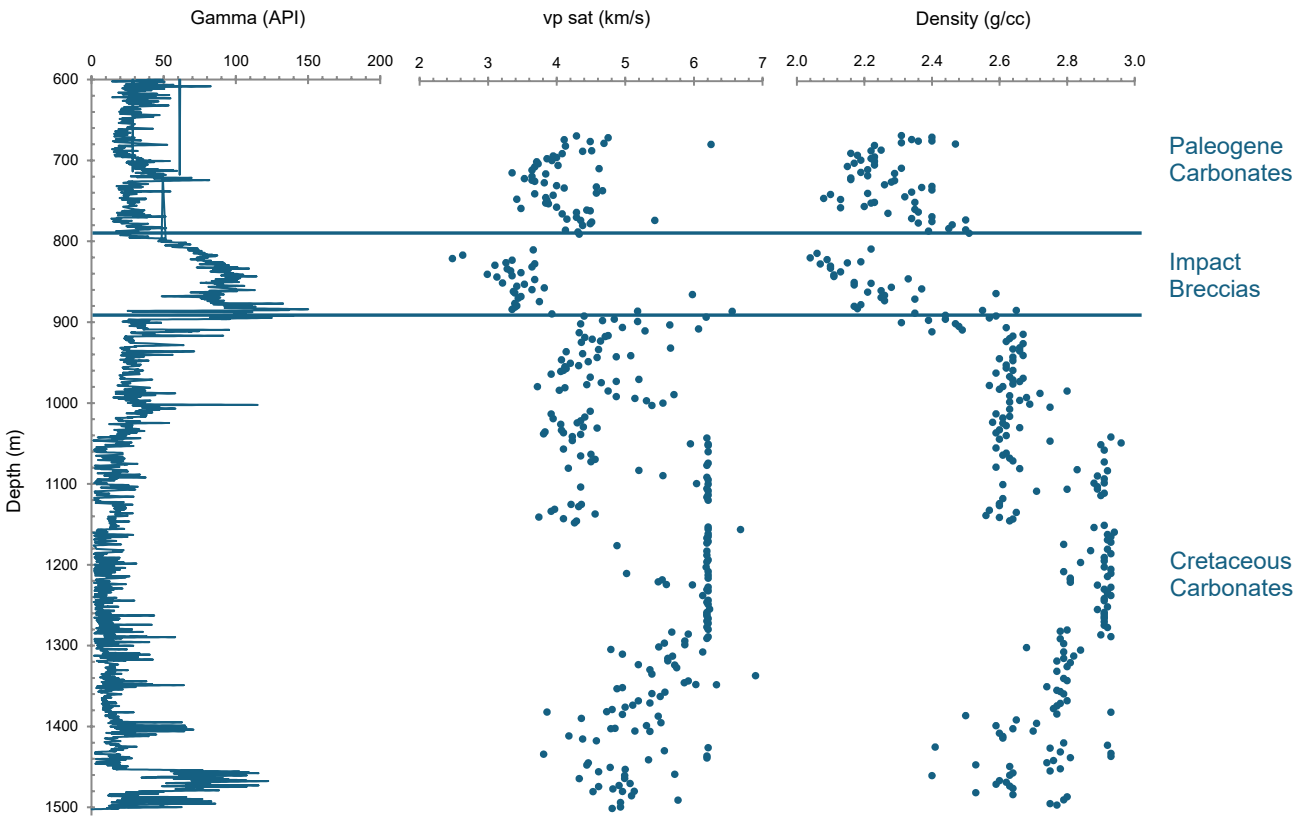

FIGURE 10. Geophysical logging for the section 600 to 1511m depth, with the gamma ray, density and seismic Vp velocity logs of post-impact carbonates, impact breccias and target carbonates (Elbra and Pesonen, 2011; Mayr *et al.*, 2008; Popov *et al.*, 2004; Wohlgemuth *et al.*, 2004).

angles downhole with superimposed internal deformation of the sequence. The core scan images permit to further evaluate relations of structural features to the impact deformation (Fig. 15). This is the case of fractures parallel to polymictic dykes and those crosscutting the dykes. The distinct structural features distinguish three major block units in the Cretaceous section, with apparent relative differential motion (Kenkmann *et al.*, 2004; Wittmann *et al.*, 2004).

In addition to the 3-D scans of core surfaces, core structures are imaged on the working core halves (Fig. 6). Scans provide continuous images of the stratigraphy, lithology, and depositional and structural features of the post-impact and target carbonates and the breccias. The core scans are also useful in the operation of the core repository for characterizing and handling fragile and damaged cores and for additional details related to the subsample analyses of the working cores.

The basement in the M0077A borehole is deformed and fractured. Dynamic collapse models and numerical simulations show crustal uplift at crater collapse stage (Baker *et al.*, 2016; Collins *et al.*, 2020). The peak ring succession in M0077A is characterized by low seismic velocities and densities and higher porosity, with a narrow 0.1 to 0.2km thick low-velocity zone of suevites and melt (Christeson *et al.*, 2018). The acoustic logs, correlated to the magnetic field measurements from the 3-component magnetometer permit to associate structural features in the cores and drill walls (Lofi *et al.*, 2018). The cores are analyzed by x-ray CT scanning using a high-energy 135kV beam and a low-energy 80kV beam to estimate density and atomic number (Gulick *et al.*, 2017; McCall *et al.*, 2020). The CT scans image the fractures and vein filling materials (Figs. 16; 17) and can be correlated to acoustic borehole images acquired on the borehole wall by ultrasonic pulses measuring the amplitude and two-way traveltime (Gulick *et al.*, 2017; Lofi *et al.*, 2018). The analyses constrain the core azimuthal orientation, which is useful for paleomagnetic, structural and stress field analyses (Paulsen *et al.*, 2002). McCall *et al.* (2021) estimated the orientations of planar cataclasite and ultraclasite zones in the granites, finding two distinct orientations with radial and tangential directions for the deformation zones. The orientations are associated with the peak ring formation and differential transport of crustal material.

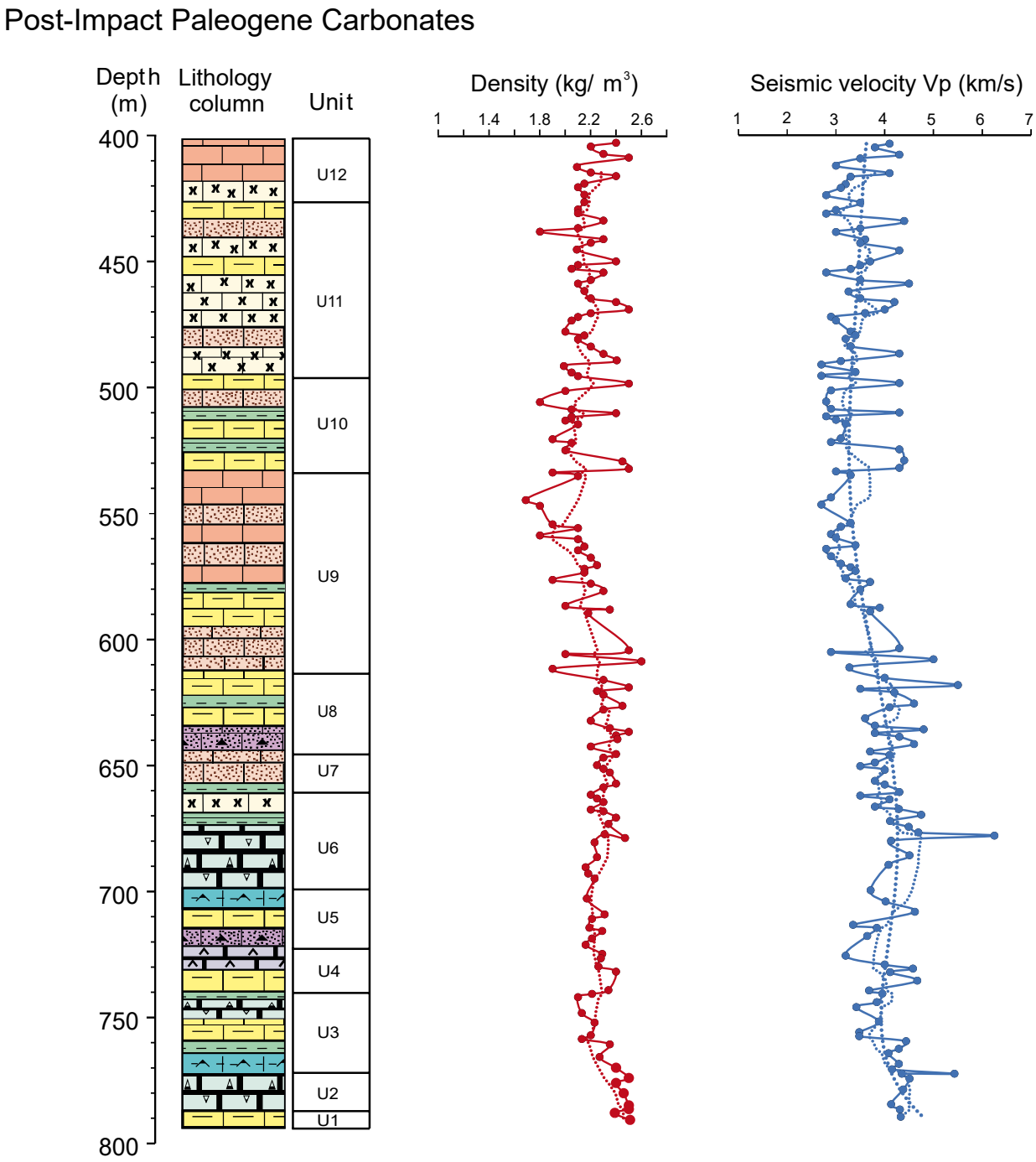

FIGURE 11. Post-impact carbonates (Escobar-Sanchez, 2018; Whalen *et al.*, 2014). Geophysical logs for the Paleogene carbonates with the density and seismic Vp velocity logs (Wohlgemuth *et al.*, 2004).

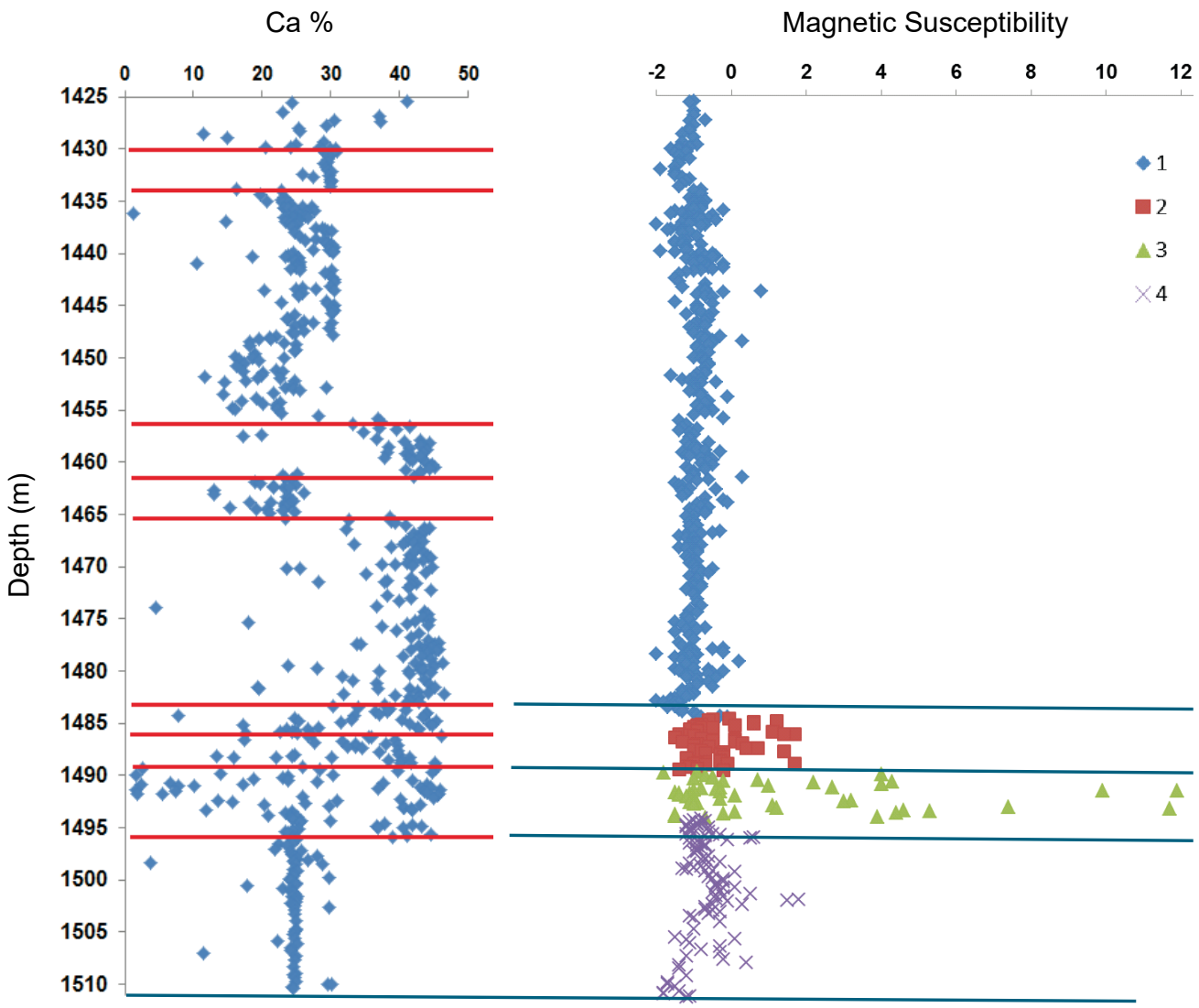

FIGURE 12 Geophysical logging for the basal section of the target carbonate sequence with the Ca chemical log and the magnetic susceptibility.

The correlations of borehole data with geophysical surveys provide constraints on the structure and stratigraphy at different scales (Gulick *et al.*, 2013). The marine seismic surveys have imaged the crater sedimentary sequence, permitting seismic stratigraphic analyses. Bell *et al.* (2004) analyzed the regional profiles Chic-A, Chic-A1, Chic-B and Chic-C, providing a basin wide view. The crater infill deposits show asymmetric distribution, with depositional changes associated with sea level changes and basin structure (Fig. 18). The basin floor marked by the top of the breccia and basal carbonate sediments is about 700m deeper than sites outside the crater, providing constraints on the K/Pg boundary horizon.

The Yaxcopoil-1 lithostratigraphic column has been correlated with the seismic images, assuming radial symmetries. Bell *et al.* (2004) correlated the borehole on the western sector and documented a thin early Paleogene section and a mid-Miocene marine regression. Whalen *et al.* (2013) correlated a revised Yaxcopoil-1 column proposing that the stratigraphy fitted the seismic packages on the eastern sector. The basin in-filling was asymmetric with distinct stratigraphic sequences on the west and east, including that western sector filled earlier. Our analysis supports a correlation of the Yaxcopoil-1 column with the western marine zone, in agreement with Bell *et al.* (2004)'s analyses. Following the crater collapse, tsunamis and debris flows affected the crater floor. Seismic reflectors delimit packages that follow the crater floor bathymetry. The marine regression on the eastern sector is followed by downlap and onlap sequences.

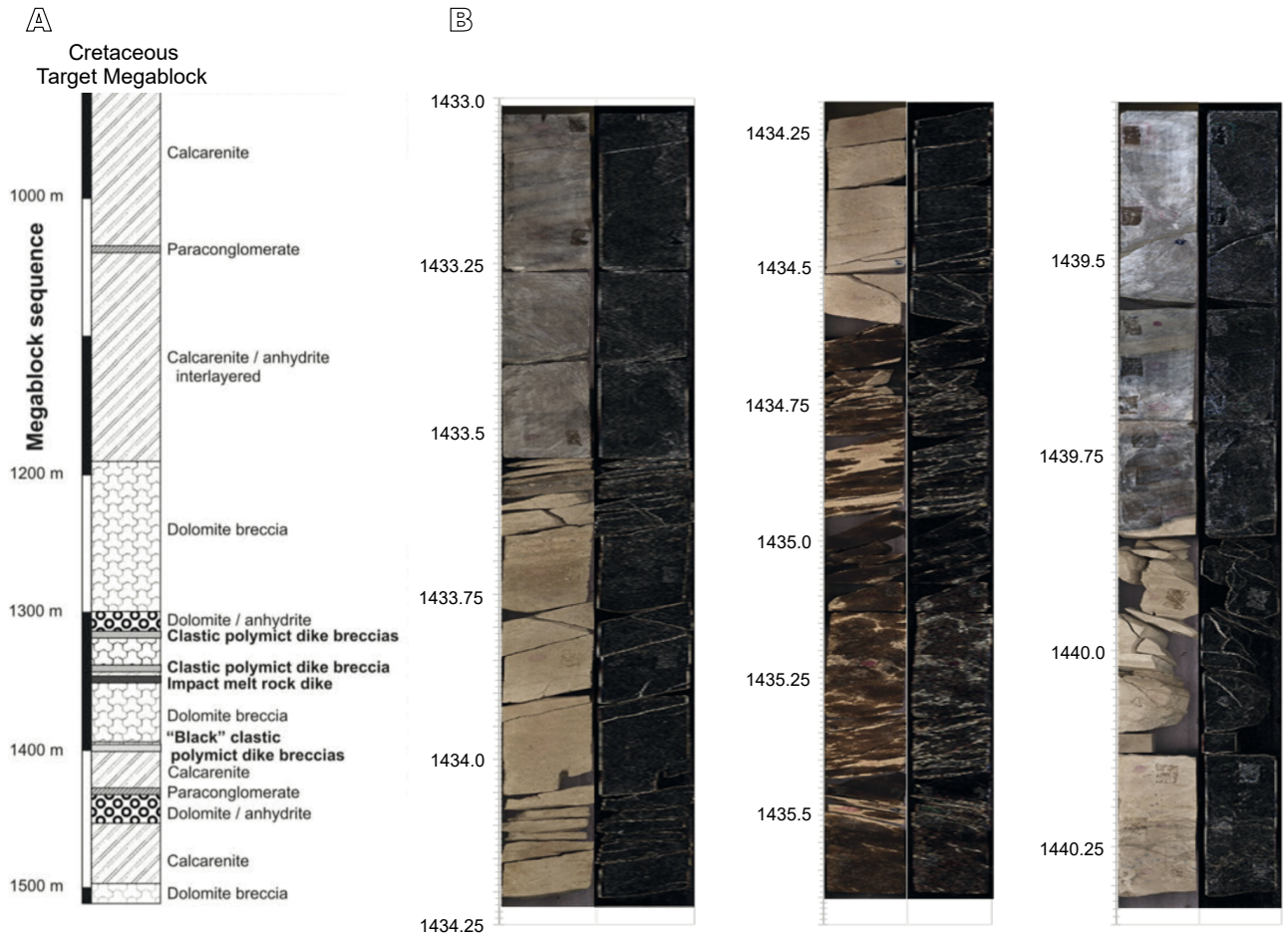

FIGURE 13. Core images in the target carbonate interval. A) Borehole column of target section with the lithological units (after Wittmann *et al.*, 2004). B) Core images of split core sections.

The borehole correlations with the seismic images have been examined considering seismic attributes (Salguero-Hernandez *et al.*, 2020). The instantaneous frequency and phase attributes enhance the seismic reflectors, characterizing the subsurface structure and stratigraphy. For the correlation, borehole lithological columns were radially rotated in the central sector (Fig. 18). The correlations are constrained from 3-D seismic and vertical seismic profile studies on the crater central zone that delineate reflector horizons and basin structure (Barton *et al.*, 2010; Canales-Garcia *et al.*, 2018; Gulick *et al.*, 2013; Nixon *et al.*, 2022; Salguero-Hernandez *et al.*, 2020).

The vertical seismic profile on the M0077A borehole provides detailed high-resolution data on the peak ring succession. In the analysis, Nixon *et al.* (2022) used the wavefield to image the structure, integrating the shear wave velocities and core data on the sonic, density, Vp/Vs ratios and elastic property logs. The carbonate sediments show a well-defined layered succession, with a strong reflector at the contact with the impactites. The impactite section shows significant scattering with anomalous low elastic impedance. The basement section shows anomalous high elastic properties, associated with the strong deformation and fracturing. Riller *et al.* (2018) associated the brittle and viscous deformation with acoustic fluidization, followed by localized microfracturing.

The peak ring units show anomalous physical properties, with low seismic velocities and densities, which are reflected in the gravity and seismic data (Christeson *et al.*, 2018; Morgan *et al.*, 2016). Christeson *et al.* (2022) modeled the seismic reflection data across the central crater zone and peak ring, integrating well logs and core analyses. They estimate that 7-75% of the melt is in the central crater zone, with a thickness above 500m thinning towards the crater rim. The peak ring shows varying topographic elevation, correlated with the average width with lower elevations over wider zones. The low velocities in the impactite section are associated with the emplacement mode and effects ocean

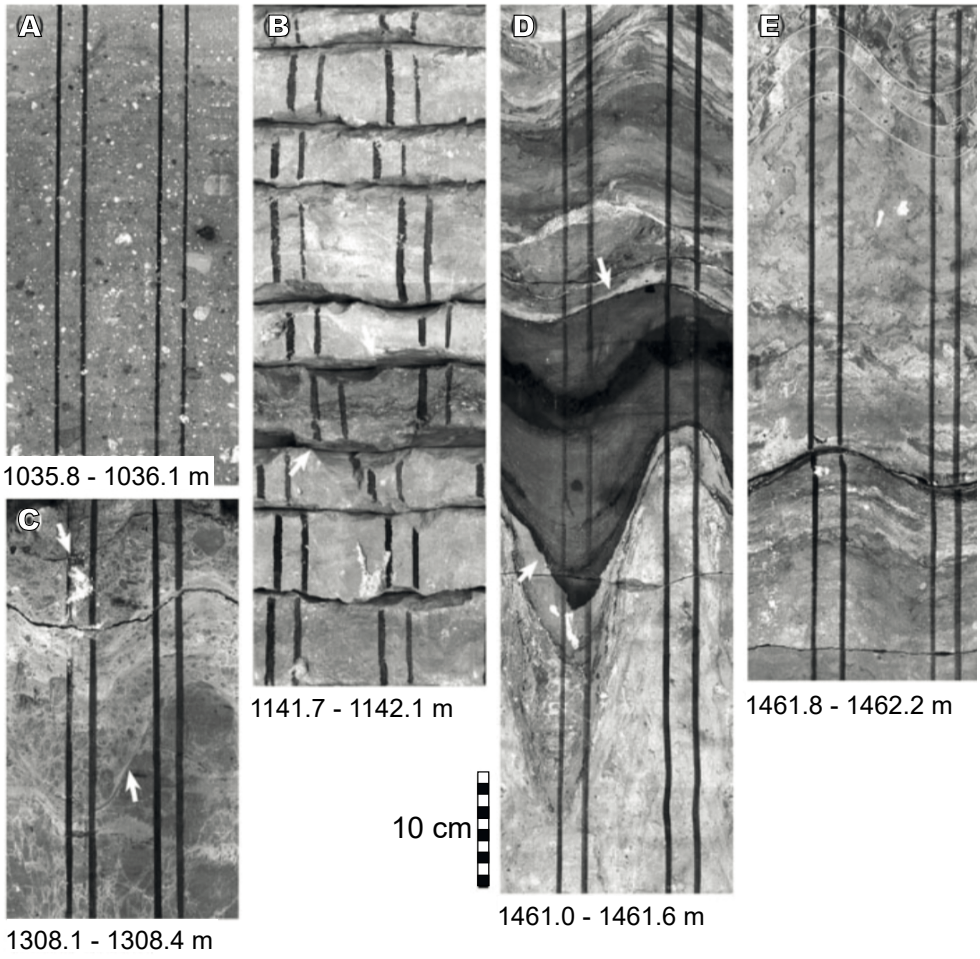

FIGURE 14. Core scan images of structural features in the target carbonate cores (after Kenkmann *et al.*, 2004). A) decoupling horizons in the paraconglomerate, B) Horizontal core breakouts at the decoupling horizons. C) Faulted breccias and discordant lithological contacts. D) Steep angle discordance and sheer planes. E) Sliding on bedding planes.

disturbance, with the graded suevite and thin melt layer emplaced over the peak ring. The models characterize the subsurface structure, with the post-impact carbonates, breccias and melt units.

CONCLUSIONS

Core scans, well logs and physical property analyses in the Yaxcopoil-1 and M0077A boreholes are used for borehole characterization and structural and stratigraphic studies. The boreholes sample distinct crater structures and stratigraphy of the terrace zone and the peak ring, which allow to constrain the crater formation process.

The Yaxcopoil-1 borehole was continuously cored from 404 to 1511m, sampling the post-impact carbonates, impact breccias and target Cretaceous carbonates. The M0077A borehole was continuously cored from 506m to 1336m, sampling the post-impact carbonates, breccias, melt and the basement section. The well logs and core analyses characterize the lithologies and physical and chemical properties of the crater units, unraveling the heterogeneous nature of the impact breccias and melt and the impact-induced deformation and hydrothermal alteration of the post-impact and target carbonates.

The digital core scans and geochemical and physical property logs characterize the stratigraphy, composition, textures fracturing and deformation. Impact breccias are heterogeneous materials with clasts of melt, carbonates and basement in carbonate-rich and melt-rich matrix. The lower breccias were emplaced by hot turbulent basal surges, followed by collapse of the impact plume and lateral curtains. The upper breccias are reworked deposits at the post-collapse stage. The logs and core analyses document that the target deformed carbonates are part of the megablock unit, displaced outwards during the crater collapse stage.

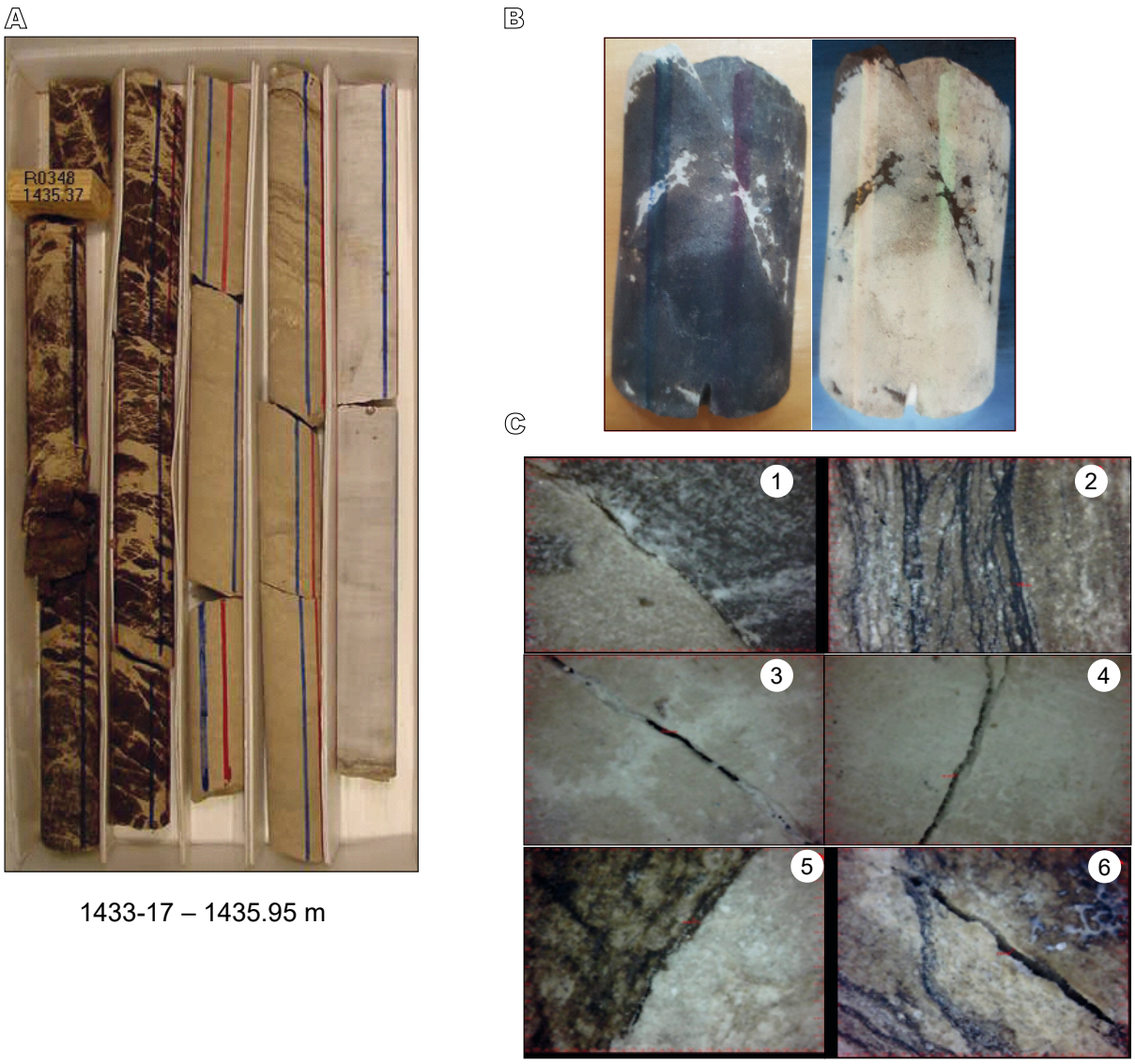

FIGURE 15. Fractures in the target carbonates show a wide range of lengths and thickness, with calcite infillings. A) representative microscope images of fractures. B) core box image of the oil-impregnated interval. C) fracture in the oil-impregnated interval.

Continuous core recovery, logging and core analyses provide detailed lithological and stratigraphic data. The cores, cuttings and fluid samples provide rich archives of information on the structure and stratigraphy. The drawbacks include long drilling time, coring tools and high costs.

The core scans and physical property analyses allow characterizing the drilled column and provide constraints on logging, borehole correlations, seismic stratigraphies and geophysical models.

CONFLICT OF INTEREST

Authors report no known conflict of interest.

ACKNOWLEDGMENTS

We greatly acknowledge Dr. Axel Wittmann, journal reviewers and editor Dr. Juan Alcalde for the useful comments on the article. We thank the IODP, ICDP and ECORD international programs for assistance with the projects. The UNAM, Government of Yucatan, Hacienda Yaxcopoil, Universidad Autonoma de Yucatan and PEMEX provided logistic support. Financial support from the Chicxulub Science Foundation grant FCC-23-002 is acknowledged. We thank the assistance and contributions to the drilling project by technicians, students and colleagues. We thank Marysol Valdez, Miguel Diaz and the Chicxulub Core Analysis Laboratory. This contribution is part of the Chicxulub Research Program and IICEAC-2024-010.

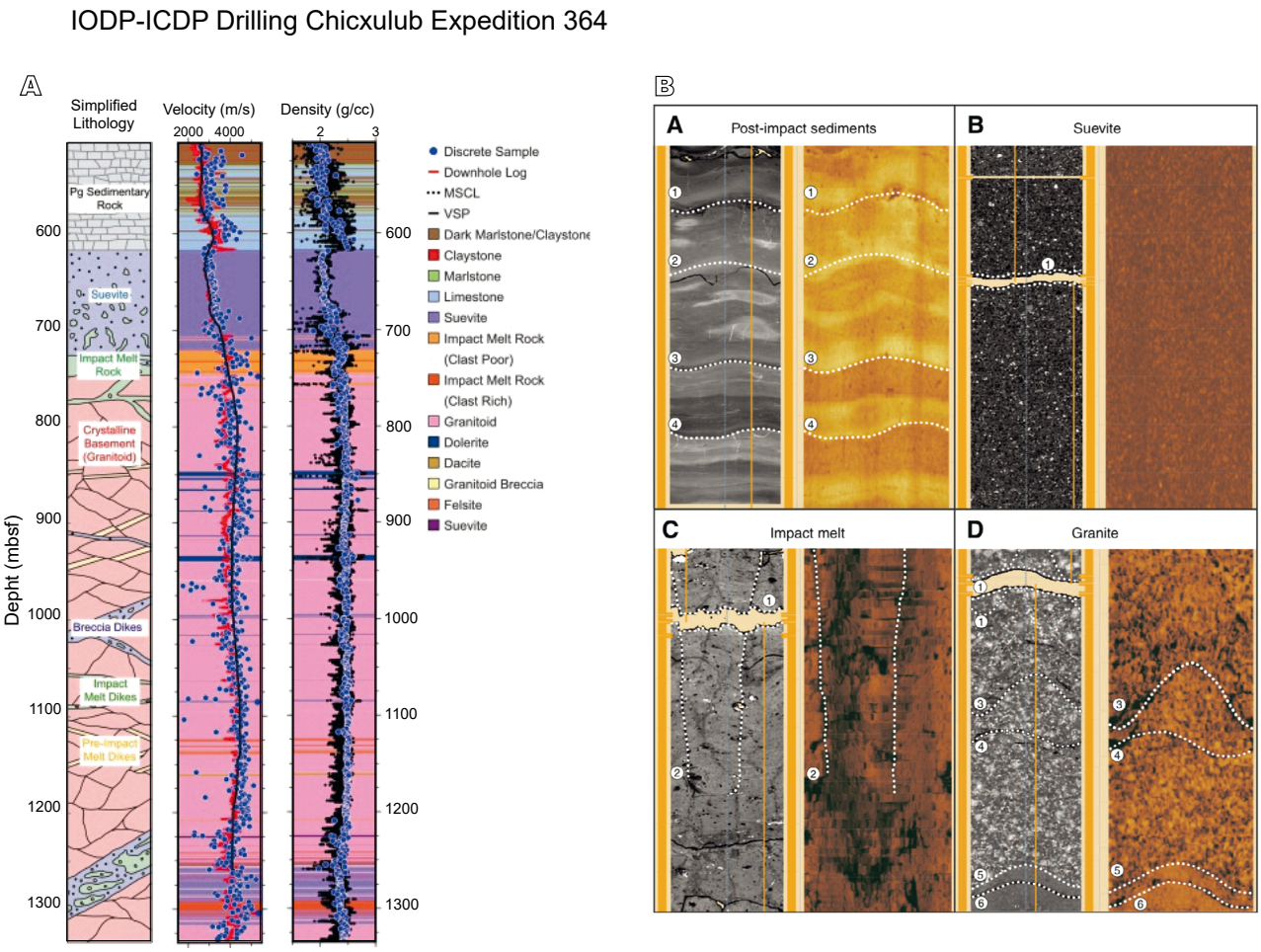

FIGURE 16. IODP-ICDP Chicxulub Drilling Expedition 364 with the M0077A borehole drilled on the peak ring. A) Borehole simplified column and the seismic velocity and density logs (from Gulick *et al.*, 2017; Morgan *et al.*, 2016). B) CT scans for the post-impact sediments, melt, suevite and basement granites with rotational values and depths of matching features in the adjusted CT scans (taken from McCall *et al.*, 2020).

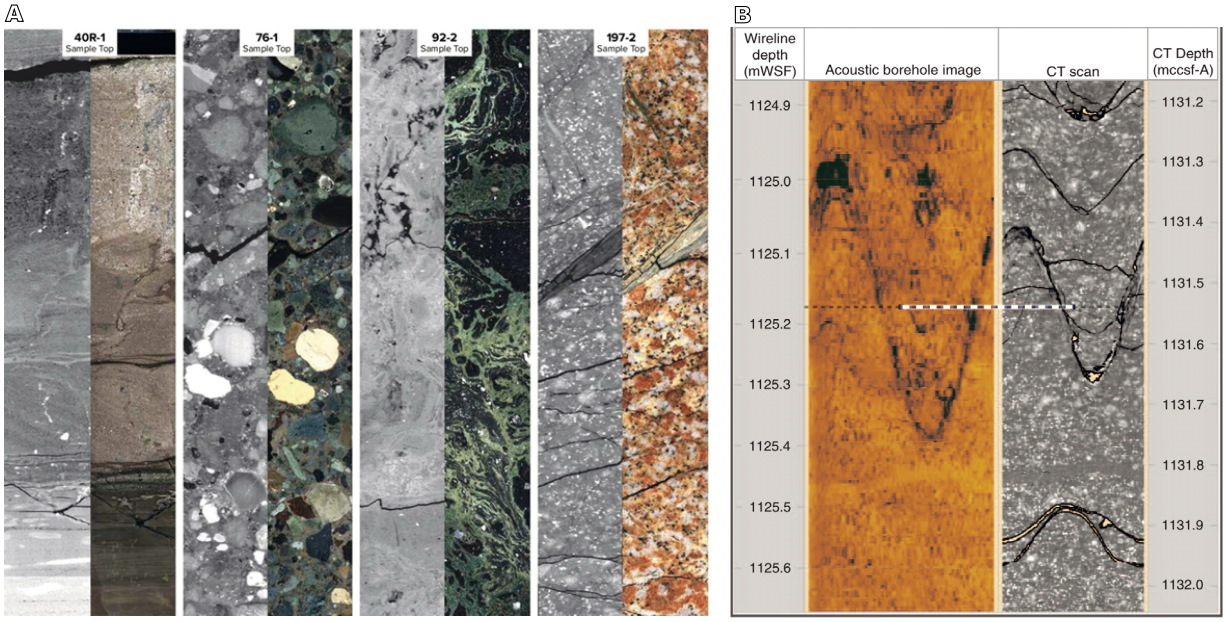

FIGURE 17. CT scans for cores of the peak ring basement granitic section at the M0077A borehole (taken from McCall *et al.*, 2020). A) CT scans for cores 40R, 76-1, 92-2 and 197-1 in the different lithologies. B) Correlation of the CT core scan and the acoustic borehole image (Gulick *et al.*, 2017; McCall *et al.*, 2020).

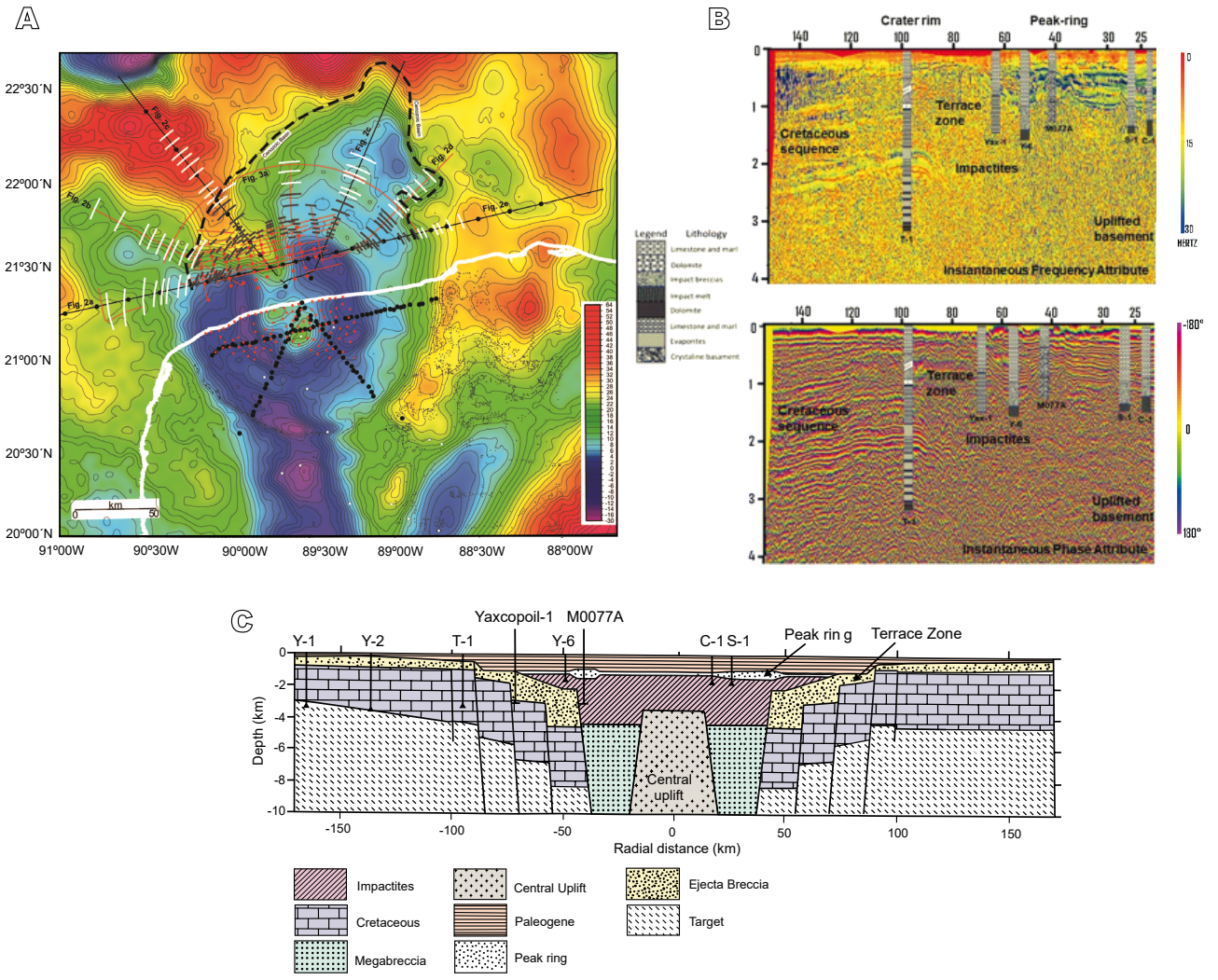

FIGURE 18. Correlation of borehole columns with the seismic data. A) Seismic line surveys plotted on the gravity anomaly (Gulick *et al.*, 2008, 2013). B) Borehole columns plotted on the instantaneous frequency and phase seismic attributes images for a sector of the E-W regional Chicx-A1 profile (taken from Salguero-Hernandez *et al.*, 2020). C) Drilling boreholes plotted on the schematic cross section of the Chicxulub impact crater showing the crater basin, central uplift, terrace zone, crater rim and the impactite deposits (taken after Hildebrand *et al.*, 1998).

REFERENCES

Akin, S., Kovscek, A.R., 2003. Computed tomography in petroleum engineering research. London, The Geological Society, 215(1, Special Publications), 23-38.

Alvarez, L.W., Alvarez, W., Asaro, F., Michel, H.V., 1980. Extraterrestrial cause for the Cretaceous–Tertiary extinction. Science, 208, 1095-1108.

Arns, C.H., Bauget, F., Sakellariou, A., Senden, T.J., Sheppard, A.P., Sok, R.M., Ghous, A., Pinczewski, W.V., Knackstedt, M.A., Kelly, J.C., 2005. Digital core laboratory: Petrophysical analysis from 3D imaging of reservoir core fragments. Petrophysics-The SPWLA Journal of Formation Evaluation and Reservoir Description, 46(04).

Artemieva, N., Morgan, J., 2020. Global K-Pg layer deposited from a dust cloud. Geophysical Research Letters, 47(6), e2019GL086562.

Arz, J.A., Alegret, L., Arenillas, I., 2004. Foraminiferal biostratigraphy and paleoenvironmental reconstruction at Yaxcopoil-1 drill hole, Chicxulub crater, Yucatán Peninsula. Meteoritics Planetary Science, 39, 1099-1112.

Ashena, R., Thonhauser, G., 2018. Coring Methods and Systems. Berlin, Springer, 243.

Aspaugh, E., 2014. Impact origin of the Moon? Annual Review Earth Planetary Sciences, 42, 551-578.

Baker, D.M.H., Head, J.W., Collins, G.S., Potter, R.W.K., 2016. The formation of peak-ring basins: Working hypotheses and path forward in using observations to constrain models of impact-basin formation. Icarus, 273, 146-163.

Barton, P.J., Grieve, R.A.F., Morgan, J.V., Surendra, A.T., Vermeesch, P.M., Christeson, G.L., Gulick, S.P.S., Warner, M.R., 2010. Seismic images of Chicxulub impact melt sheet and comparison with the Sudbury structure. Geological Society of America, 465 (Special Paper), 103-113.

Batista, J., Pérez-Flores, M.A., Urrutia-Fucugauchi, J., 2013. Three-dimensional gravity modeling of Chicxulub crater structure, constrained with marine seismic data and land boreholes. Earth Planets Space, 65, 973-983.

Becker, K., Davis, E.E., 2005. A review of CORK designs and operations during the Ocean Drilling Program. In: College Station, TX, USA. Proceedings Integrated Ocean Drilling Program, 301,.

Becker, K., Austin, J.A., Exon, N., Humphris, S., Kastner, M., McKenzie, J.A., Miller, K.G., Suyehiro, K., Taira, A., 2019. 50 Years of Scientific Ocean Drilling. Oceanography, 32(1), 17-21.

Bell, C., Morgan, J., Hampson, G.J., Trudgill, B., 2004. Stratigraphic and sedimentological observations from seismic data across the Chicxulub impact basin. Meteoritics Planetary Science, 39, 1089-1098.

Canales-Garcia, I., Urrutia-Fucugauchi, J., Aguayo-Camargo, E., 2018. Seismic imaging and attribute analysis of Chicxulub crater central sector, Yucatan platform, Gulf of Mexico. Geologica Acta, 16(2), 215-235.

Chapman, R.E., 2000. Petroleum Geology. Elsevier.

Christeson, G.L. et al., 2018. Extraordinary rocks from the peak ring of the Chicxulub impact crater: P-wave velocity, density and porosity measurements from IODP/ICDP Expedition 364. Earth Planetary Science Letters, 495, 1-11.

Christeson, G.L., Morgan, J.V., Gulick, S.P.S., 2021. Mapping the Chicxulub impact stratigraphy and peak ring using drilling and seismic data. Journal of Geophysical Research: Planets, 126(8), e2021JE006938.

Collins, G.S., Morgan, J., Barton, P., Christeson, G.L., Gulick, S., Urrutia Fucugauchi, J., Warner, M., Wünnemann, K., 2008. Dynamic modeling suggests terrace zone asymmetry in the Chicxulub crater is caused by target heterogeneity. Earth and Planetary Science Letters, 270(3-4), 221-230.

Collins, G.S., Patel, N., Davison, T.M., Rae, A.S., Morgan, J.V., Gulick, S. et al., 2020. A steeply-inclined trajectory for the Chicxulub impact. Nature Communications, 11(1), 1480.

Conze, R., 2016. Drilling Information System (DIS) and Core Scanner. Journal of large-scale research facilities Journal Large Scale RF, 2, A63-A63.

Conze, R., Wallrabe-Adams, H.J., Graham, C. Krysiak, F., 2007. Joint data management on ICDP projects and IODP Mission Specific Platform Expeditions. Scientific drilling, 4, 32-34.

Delgado-Rodríguez, O.D., Enríquez, O.C., Urrutia-Fucugauchi, J., Arzate, J.A., 2001. Occam and Bostick 1-D inversion of magnetotelluric soundings in the Chicxulub impact crater, Yucatan, Mexico. Geofisica Internacional, 40(4), 271-283.

Duong, T.N.M., Hernawan, B., Medina-Zetina, Z., Urrutia-Fucugauchi, J., 2023. Numerical modeling of an asteroid impact on Earth: Matching field observations at the Chicxulub crater using the distinct element method (DEM). Geosciences, 13(5), 139. DOI: 10.3390/geosciences13050139

Elbra, T., Pesonen, L.J., 2011. Physical properties of the Yaxcopoil-1 deep drill core, Chicxulub impact structure, Mexico. Meteoritics & Planetary Science, 46(11), 1640-1652.

Escobar-Sánchez, J.E., Urrutia-Fucugauchi, J., 2010. Chicxulub crater post-impact hydrothermal activity - evidence from Paleocene carbonates in the Santa Elena borehole. Geofisica Internacional, 49, 97-106.

Freifeld, B.M., Kneafsey, T.J., Rack, F.R., 2006. On-site geological core analysis using a portable X-ray computed tomographic system. London, The Geological Society, 267(1, Special Publications), 267(1), 165-178.

French, C.D., Schenk, C.J., 2004. Map showing geology, oil and gas fields, and geologic provinces of the Caribbean region. US Geological Survey Open-File Report 97-470-K, CD-ROM.

García-Garnica, E.M., Pérez-Cruz, L., 2022. Hyperthermal events recorded in the Palaeogene carbonate sequence of southern Gulf of Mexico—Santa Elena borehole, Yucatan Peninsula. Geological Journal, 57(1), 99-113.

Gelinas, A., Kring, D.A., Zurcher, L., Urrutia-Fucugauchi, J., Morton, O., Walker, R.J., 2004. Osmium isotope constraints on the proportion of bolide component in Chicxulub impact melts. Meteoritics and Planetary Science, 39, 1003-1008.

Goff, J.A., Gulick, S.P., Cruz, L.P., Stewart, H.A., Davis, M., Duncan, D., Saustrup, S., Sanford, J., Urrutia-Fucugauchi, J., 2016. Solution pans and linear sand bedforms on the bare-rock limestone shelf of the Campeche Bank, Yucatán Peninsula, Mexico. Continental Shelf Research, 117, 57-66.

Gulick, S., Barton, P., Christeson, G., Morgan, J., MacDonald, M., Mendoza, K., Urrutia-Fucugauchi, J., Vermeesch, P., Warner, M., 2008. Importance of pre-impact crustal structure for the asymmetry of the Chicxulub impact crater. Nature Geoscience, 1, 131-135.

Gulick, S.P.S., Christeson, G.L., Barton, P.J., Grieve, R., Morgan, J., Urrutia-Fucugauchi, J., 2013. Geophysical characterization of the Chicxulub impact crater. Reviews of Geophysics, 51, 31-52.

Gulick, S., Morgan, J., Mellett, C.L., Green, S.L., Bralower, T., Chenot, E., Christeson, G., Claeys, P., Cockell, C., Coolen, M., Ferriere, L., Gebhardt, C., Goto, K., Jones, H., Kring, D., Lofi, J., Lowery, C., Ocampo-Torres, R., Perez-Cruz, L., Pickersgill, A.E., Poelchau, M., Rae, A., Rasmussen, C., Rebolledo, M., Riller, U., Sato, H., Smit, J., Tikoo, S., Tomioka, N., Urrutia-Fucugauchi, J., Whalen, M., Wittmann, A., Yamaguchi, K., Xiao, L., Zylberman, W., 2017. Expedition 364 Site M0077. In: Morgan, J., Gulick, S., Mellett, C.L., Green, S.L. (eds.). Proceedings of the International Ocean Discovery Program, 364.

Harms, U., Emmermann, R., 2017. History and Status of the International Continental Drilling Program. In: Harms, U. et al. (eds.). Continental Scientific Drilling. Springer, 366.

Hildebrand, A.R., Penfield, G.T., Kring, D.A., Pilkington, M., Camargo-Zanoguera, A., Jacobsen, S.B., Boynton, W.V., 1991. Chicxulub Crater: A possible Cretaceous/Tertiary boundary impact crater on the Yucatan Peninsula, Mexico. Geology, 19, 867-871.

Hildebrand, A., Pilkington, M., Ortiz-Aleman, C., Chavez, R., Fucugauchi, J., Connors, M., Graniel-Castro, E., Camara-Zi, A., Niehaus, J., 1998. Mapping Chicxulub crater structure

with gravity and seismic data. In: Meteorites: Flux with Time and Impact Effects, Grady, R. et al. (eds.). Geological Society Special Publication, 140, 155-176.

Kenkmann, T., 2021. The terrestrial impact crater record: A statistical analysis of morphologies, structures, ages, lithologies, and more. Meteoritics & Planetary Science, 56(5), 1024-1070.

Kenkmann, T., Wittmann, A., Scherler, D., 2004. Structure and impact indicators of the Cretaceous sequence of the ICDP drill core Yaxcopoil-1, Chicxulub impact crater, Mexico. Meteoritics Planetary Science, 39, 1069-1088.

Kenkmann, T., Poelchau, M.H., Wulf, G., 2014. Structural geology of impact craters. Journal of Structural Geology, 62, 156-182.

Keppie, J.D., Dostal, J., Norman, M., Urrutia-Fucugauchi, J., Grajales-Nishimura, M., 2011. Study of melt and a clast of 546 Ma magmatic arc rocks in the 65 Ma Chicxulub bolide breccia, northern Maya block, Mexico: western limit of Ediacaran arc peripheral to northern Gondwana. International Geology Review, 53(10), 1180-1193.

Kring, D.A., Horz, L., Zurcher, L., Urrutia-Fucugauchi, J., 2004. Impact lithologies and their emplacement in the Chicxulub impact crater: Initial results from the Chicxulub scientific drilling project, Yaxcopoil, Mexico. Meteoritics Planetary Science, 39, 879-897.

Lofi, J., Smith, D., Delahunty, C., Le Ber, E., Brun, L., Henry, G., Paris, J., Tikoo, S., Zylberman, W., Pezard, P.A. Célérier, B., Expedition 364 Science Party, 2018. Drilling-induced and logging-related features illustrated from IODP–ICDP Expedition 364 downhole logs and borehole imaging tools. Scientific Drilling, 24, 1-13.

Lopez Ramos, E., 1976. Geological summary of the Yucatan peninsula. In: Nairn, A.E.M., Stehli, F.G. (eds.). The Ocean Basins and Margins, 3, The Gulf of Mexico and the Caribbean. New York, Plenum, 257-282.

Lüders, V., Rickers, K., 2004. Fluid inclusion evidence for impact-related hydrothermal fluid and hydrocarbon migration in Cretaceous sediments of the ICDP-Chicxulub drill core Yax-1. Meteoritics Planetary Science, 39(7), 1187-1197.

Mayr, S.I., Wittmann, A., Burkhardt, H., Popov, Y., Roumushkevich, R., Bayuk, I., Heidinger, P., Wilhelm, H., 2008. Integrated interpretation of physical properties of rocks of the borehole Yaxcopoil-1 (Chicxulub impact structure). Journal Geophysical Research, 113, B7201.

McCall, N., Gulick, S., Hall, B., Lofi, J. Poelchau, M., 2020. Data report: Orientation correction of Chicxulub core recovered from IODP/ICDP Expedition 364. Proceedings of the International Ocean Discovery Program, 364.

McCall, N., Gulick, S.P., Hall, B., Rae, A.S., Poelchau, M.H., Riller, U., Lofi, J., Morgan, J.V., 2021. Orientations of planar cataclasite zones in the Chicxulub peak ring as a ground truth for peak ring formation models. Earth Planetary Science Letters, 576, 117236.

Melosh, H.J., 1989. Impact Cratering: A Geologic Process. New York, Oxford University Press, 245.

Melosh, H.J., B.A. Ivanov, 1999. Impact crater collapse. Annual Reviews Earth Planetary Sciences, 385-415.

Morgan, J., Warner, M., Chicxulub group, 1997. Size and morphology of the Chicxulub impact crater. Nature, 390, 472-476.

Morgan, J., Urrutia-Fucugauchi, J., Gulick, S., Christeson, G., Barton, P., Rebolledo-Vieyra, M., Melosh, J., 2005. Chicxulub crater seismic survey prepares way for future drilling. Eos, Transactions American Geophysical Union, 86(36), 325-328.

Morgan, J., Gulick, S., Bralower, T., Chenot, E., Christen, G., Claeys, P., Cockell, C., Collins, G., Coolen, M., Ferrière, L., Gebhardt, C., Goto, K., Jones, H., Kring, D., Le Ber, E., Lofi, J., Long, X., Lowery, C., Mellet, C., Ocampo-Torres, R., Osinski, G., Perez-Cruz, L., Pickersgill, A., Pölchau, M., Rae, A., Rasmussen, C., Rebolledo-Vieyra, M., Riller, U., Sato, H., Schmitt, D., Smit, J., Tikoo-Schantz, S., Tomioka, N., Fucugauchi, J.U., Whalen, M., Wittmann, A., Yamaguchi, K., Zylberman, W., 2016. The formation of peak rings in large impact craters. Science, 354, 878-882.

Morgan, J., Gulick, S., Mellet, C.L., Green, S.L., Expedition 364 Scientists, 2017. Chicxulub: Drilling the K-Pg impact crater. Proceedings International Ocean Discovery Program, 364, College Station TX DOI: https:doi.org/10.14379/iodp.proc.364.2017.

Moon, C.J., Whateley, M.K., Evans, A.M., 2006. Introduction to Mineral Exploration. Blackwell publishing, 2nd edition .

National Research Council, 1994. Drilling and excavation technologies for the future. Division on Earth, Life Studies, Commission on Geosciences and Committee on Advanced Drilling Technologies, National Academies Press.

Nixon, C.G., Schmitt, D.R., Kofman, R., Lofi, J., Gulick, S.P., Saustrup, S., Christeson, G.L., Kring, D.A., 2022. Borehole seismic observations from the Chicxulub impact drilling: Implications for seismic reflectivity and impact damage. Geochemistry, Geophysics, Geosystems, 23(3), p.e2021GC009959.

Paulsen, T.S., Jarrard, R.D., Wilson, T.J., 2002. A simple method for orienting drill core by correlating features in whole-core scans and oriented borehole-wall imagery. Journal of Structural Geology, 24(8), 1233-1238.

Perez-Cruz, L., Urrutia-Fucugauchi, J., 2024. Chicxulub's legacy: Breakthroughs from scientific drilling, tsunamis, global climate upheaval and mass extinction. Past Global Changes Magazine, 32(2), 82-83. DOI: https://doi.org/10.22498/pages.32.82

Pilkington, M., Ames, D.E. Hildebrand, A.R., 2004. Magnetic mineralogy of the Yaxcopoil-1 core, Chicxulub. Meteoritics Planetary Science, 39(6), 831-841.

Pope, K.O., Ocampo, A.C., Fischer, A.G., Vega, F.J., Ames, D.E., King, D.T., Jr., Fouke, B.W., Wachtman, R.J., Kletetschka, G., 2005. Chicxulub impact ejecta deposits in southern Quintana Roo, México, and central Belize. In: Kenkmann, T., Hörz, F., Deutsch, A. (eds.). Large meteorite impacts III. Geological Society of America, 384 (Special Paper), 171-190.

Popov, Y., Romushkevich, R., Bayuk, I., Korobkov, D., Mayr, S., Burkhardt, H., Wilhelm, H., 2004. Physical properties of rocks

from the upper part of the Yaxcopoil-1 drill hole, Chicxulub crater. Meteoritics Planetary Science, 39, 799-812.l

Revelle, R., 1981. The past and future of scientific ocean drilling. In: Warme *et al.*, J.E. (eds.). The Deep Sea Drilling Project: A Decade of Progress. SEPM, 32 (Special Publication), .

Riller, U., Poelchau, M.H., Rae, A.S.P., Schulte, F.M., Collins, G.S., Melosh, H.J., et al. 2018. Rock fluidization during peak-ring formation of large impact structures. Nature, 562(7728), 511-518. DOI: https://doi.org/10.1038/s41586-018-0607-z

Rothwell, R.G., Rack, F.R., 2006. New techniques in sediment core analysis: an introduction. London, The Geological Society, 267(1, Special Publications), 1-29.

Rowe, A.J., Wilkinson, J.J., Coles, B.J. Morgan, J.V., 2004. Chicxulub: Testing for post-impact hydrothermal input into the Tertiary ocean. Meteoritics Planetary Science, 39(7), 1223-1231.

Salguero-Hernández, E., Pérez-Cruz, L., Urrutia-Fucugauchi, J., 2020. Seismic attribute analysis of Chicxulub impact crater. Acta Geophysica, 68(3), 627-640.

Schmieder, M., Shaulis, B.J., Lapen, T.J., Kring, D.A., 2018. U–Th–Pb systematics in zircon and apatite from the Chicxulub impact crater, Yucatán, Mexico. Geological Magazine, 155(6), 1330-1350.

Schulte, P., Alegret, L., Arenillas, I., Arz, J., Barton, P., Bown, P., Bralower, T., Christeson, G., Claeys, P., Cockell, C., Collins, G., Deutsch, A., Goldin, T., Goto, K., Grajales-Nishimura, J., Grieve, R., Gulick, S., Johnson, K., Kiessling, W., Willumsen, P., 2010. The Chicxulub asteroid impact and mass extinction at the Cretaceous-Paleogene boundary. Science, 327, 1214-1218.

Selley, R.C., 1998. Elements of Petroleum Geology. San Diego (California), Academic Press, 2nd Edition,

Sharpton, V.L., Dalrymple, G., Marin, L., Ryder, G., Schuraytz, B., Urrutia-Fucugauchi, J., 1992. New links between the Chicxulub impact structure and the Cretaceous/Tertiary boundary. Nature, 359, 819-821.

Sharpton, V., Burke, K., Camargo-Zanoguera, A., Hall, S., Lee, D., Marín, L., Suáarez-Reynoso, G., Quezada-Muñeton, J., Spudis, P., Fucugauchi, J., 1993. Chicxulub multiring impact basin: Size and other characteristics derived from gravity analysis. Science, 261, 1564-1567.

Shouting, T., Wentao, W., 2022. International Scientific Ocean Drilling 2050 Science Framework and Its Implications for Future Scientific Ocean Drilling Development. Advances in Earth Science, 37(10), 1049.

Smith, N.T., Shreeve, J., Kuras, O., 2020. Multi-sensor core logging (MSCL) and X-ray computed tomography imaging of borehole core to aid 3D geological modelling of poorly exposed unconsolidated superficial sediments underlying complex industrial sites: An example from Sellafield nuclear site, UK. Journal of Applied Geophysics, 178, 104084.

Stöffler, D., Artemieva, N.A., Ivanov, B.A., Hecht, L., Kenkemann, T., Schmitt, R.T., Tagle, R.A., Wittmann, A., 2004. Origin and emplacement of the impact formations at Chicxulub, Mexico, as revealed by the ICDP deep drilling at Yaxcopoil-1 and by numerical modeling. Meteoritics Planetary Science, 39, 1035-1067.

Tanaka, A., Nakano, T., Ikehara, K., 2011. X-ray computerized tomography analysis and density estimation using a sediment core from the Challenger Mound area in the Porcupine Seabight, off Western Ireland. Earth, Planets and Space, 63, 103-110.

Tonai, S., Kubo, Y., Tsang, M.Y., Bowden, S., Ide, K., Hirose, T., Kamiya, N., Yamamoto, Y., Yang, K., Yamada, Y., Morono, Y., 2019. A new method for quality control of geological cores by X-ray computed tomography: Application in IODP expedition 370. Frontiers in Earth Science, 7, 117.

Tuchscherer, M.G., Reimold, W.U., Koeberl, C., Gibson, R.L., 2004. Major and trace element characteristics of impactites from the Yaxcopoil-1 borehole, Chicxulub structure, Mexico. Meteoritics Planetary Science, 39,

Urrutia-Fucugauchi, J., Pérez-Cruz, L., 2008. Post-impact carbonate deposition in the Chicxulub impact crater region, Yucatan platform, Mexico. Current Science, 95, 248-252.

Urrutia-Fucugauchi, J., Pérez-Cruz, L., 2011. Buried impact basins, the evolution of planetary surfaces and the Chicxulub multi-ring crater. Geology Today, 27, 222-227.

Urrutia-Fucugauchi, J., Marin, L., Trejo, A., 1996. UNAM scientific drilling program of Chicxulub impact structure – Evidence for a 300 kilometer crater diameter. Geophysical Research Letters, 23, 1565-1568.

Urrutia-Fucugauchi, J., Morgan, J., Stoeffler, D., Claeys, P., 2004. The Chicxulub scientific drilling project (CSDP). Meteoritics Planetary Science, 39, 787-790.

Urrutia-Fucugauchi, J., Chavez, J.M., Pérez-Cruz, L., de la Rosa, J.L., 2008. Impact ejecta and carbonate sequence in the eastern sector of Chicxulub Crater. Comptes Rendus Geosciences, 40, 801-810. DOI: 10.1016 /j.crte.2008.09.001

Urrutia-Fucugauchi, J., Camargo-Zanoguera, A., Pérez-Cruz, L., Pérez-Cruz, G., 2011. The Chicxulub multiring impact crater, Yucatan carbonate platform, Mexico. Geofisica Internacional, 50, 99-127.

Urrutia-Fucugauchi, J., Pérez-Cruz, L., Campos, S.E., Escobar, J.E., Velasco-Villarreal, M., 2014. Magnetic susceptibility logging of Chicxulub proximal impact breccias in the Santa Elena borehole – Implications for emplacement mode. Studia Geophysica et Geodaetica, 58, 100-120.

Urrutia-Fucugauchi, J., Arellano-Catalán, O., Pérez-Cruz, L., Romero-Galindo, I.A., 2022. Chicxulub crater joint gravity and magnetic anomaly analysis: Structure, asymmetries, impact trajectory and target structures. Pure Applied Geophysics, 179(8), 2735-2756.

Whalen, M., Gulick, S., Pearson, Z., Norris, R.D., Pérez-Cruz, L., Urrutia-Fucugauchi, J., 2013. Annealing the Chicxulub impact: Paleogene Yucatan carbonate slope development in the Chicxulub impact basin, Mexico. Society for Sedimentary Geology Special Publication, 105, 282-304. DOI: 10.2110/sepmsp.105.04

Whalen, M.T., Gulick, S.P., Lowery, C.M., Bralower, T.J., Morgan, J.V., Grice, K., Schaefer, B., Smit, J., Ormö, J., Wittmann,

A., Kring, D.A., IODP-ICDP Science Party, 2020. Winding down the Chicxulub impact: The transition between impact and normal marine sedimentation near ground zero. Marine Geology, 430, 106368.

Wittmann, A., Kenkmann, T., Schmidt, R.T., Hecht, L., Stöffler, D., 2004. Impact-related dike breccia lithologies in the ICDP drill core Yaxcopoil-1, Chicxulub impact structure, Mexico. Meteoritics Planetary Science, 39, 931-954.

Wohlgemuth, L., Bintakies, E., Kück, J., Conze, R., Harms, U., 2004. Integrated deep drilling, coring, downhole logging, and data management in the Chicxulub Scientific Drilling Project (CSDP), Mexico. Meteoritics Planetary Science, 39(6), 791-797.

Yamada, Y., Dugan, B., Hirose, T., Saito, S., 2019. Riser drilling: Access to deep subsurface science. Oceanography, 32, 95-97.

Manuscript received May 2024;
revision accepted December 2024;
published Online Februray 2025.